Hamburg University of Applied Sciences

Faculty of Life Sciences

From Waste to Sortable Material: Processing and Characterization of Recycled Glass

Bachelor-Thesis

Submitted by:

Aldiska Meivina

[redacted]

Process Engineering (*Verfahrenstechnik*)

Hamburg, 09.10.2025

First reviewer	**: Prof. Dr. Kai Freudenthal**	**(HAW Hamburg)**
Second reviewer	**: Dipl.-Ing. Marc Hannapel**	**(HAW Hamburg)**

This thesis was supervised and prepared in the laboratory of HAW Hamburg

Abstract

Recycling glass is a key step toward sustainable material use, reducing the need for virgin resources, minimising environmental impacts, and supporting circular economy goals. This thesis focuses on the preparation and characterization

of clear and green recycled glass as a foundation for future research in automated optical colour-sorting technologies.

The work demonstrates that simple, yet effective procedures are sufficient to prepare high-quality cullet at laboratory scale. Post-consumer glass was collected, cleaned with resource-efficient methods, and processed through manual and mechanical crushing. Sieving techniques were employed to achieve standardised particle size fractions, particularly in the range of 4–10 mm, which is considered optimal for optical sorting. By comparing different crushing techniques and analysing particle size distribution, the study highlights how fragmentation behaviour differs between clear and green glass and how these differences can affect sorting performance.

In addition to particle size, the thesis examines essential physical properties such as particle density, bulk and tapped density, porosity, and flow behaviour. These characteristics determine how cullets behave during handling, storage, transport, and separation, and therefore play a crucial role in recycling efficiency. A combination of manual and instrument-based methods was applied to ensure accuracy and practical relevance.

The findings underline that the crushing method and particle properties directly influence downstream processes. Excessive fines hinder sorting efficiency, while controlled fragmentation produces cullets better suited for automated systems. Overall, the study provides a comprehensive characterization of recycled glass and establishes a reproducible preparation method. In doing so, it creates a robust foundation for future research and contributes to the development of more precise, efficient, and scalable glass recycling systems.

Contents

List of Symbols

ρ	Density	[kg/m^3]
$\rho_{particle}$	Particle density	[kg/m^3]
m	Mass	[kg]
mo	Initial mass	[kg]
me	End mass	[kg]
V	Volume	[m^3]
m_{Glass}	Mass of glass sample	[kg]
$V_{particle}$	Particle volume	[m^3]
ρ_{bulk}	Bulk density	[kg/m^3]
V_{glass}	Volume of glass sample	[m^3]
ε	Porosity	[-]
$\Delta\varepsilon$	Uncertainty of porosity	[-]
δ	Relative deviation (or error)	[-]
$\Delta\rho$	Uncertainty of density	[kg/m^3]
Δm	Uncertainty of mass	[kg]
ΔV	Uncertainty of volume	[m^3]
Q3(x)	Cumulative particle size distribution	[-]
q3(x)	Differential particle size distribution	[-]
dx	Sieve interval	[mm]
x	Mesh size	[mm]
$\bar{x}$	Mean particle size/ size class	[mm]
Δp	Pressure drop	[Pa]
H	Bed height	[m]
η	Dynamic viscosity of air	[Pas]
$\bar{w}$	Superficial gas velocity	[m/s]
ρ_f	Density of air	[kg/m3]
d_{32}	Sauter mean particle diameter	[m]

List of Figures

List of Table

1. Introduction

Glass is an exceptionally versatile industrial material due to its myriad applications, durability, and inertness to chemicals (Abdelouas et al., 2019). Glass has been integral to human society for millennia and continues to play a significant role in both daily living and scientific endeavours. The initial chapter of the *Springer Handbook* of Glass states that glass persists due to its versatility and strength. Georges Bontemps stated in 1868, as cited in (Chopinet, 2019).

"Among the numerous and varied products that attest to the industrial genius of mankind, few others have as many uses as glass or possess such marvellous properties... No other material could replace glass in its most important applications; only iron could dispute the pre-eminence of this diaphanous substance."

From scientific discovery to daily use, glass facilitates humanity's ability to view the infinitesimal and the incomprehensibly remote, to store and safeguard, and also to reflect and convey. Currently, its footprint encompasses sectors like packaging, construction, automotive, and consumer products (Lebullenger et al., 2019). The distinctive characteristics of glass, especially its capacity for infinite recycling without substantial quality deterioration, make it a vital asset in resource conservation and environmental protection initiatives (Doremus, 1994). As environmental concerns escalate and societies recognise the implications of resource depletion and waste production, efficient and effective glass recycling has emerged as a critical issue for both industry and research (UNEP, 2024).

Recycling glass provides numerous environmental and financial advantages. It reduces the use of raw materials like sand, soda ash, and limestone, while also significantly decreasing energy use in the manufacture of new glass. According to a comprehensive Life Cycle Assessment (LCA) report by the European Container Glass Federation, or Fédération Européenne du Verre d'Emballage (*FEVE-Brochure-Recycling-Why-Glass-Always-Has-a-Happy-CO2-Ending*, n.d.), one tonne of recycled glass (cullet) replaces 1,2 tonnes of virgin raw material and cuts approximately 0,67 tonnes of CO_2 emissions—achieving up to a 58% reduction in furnace CO_2 emissions when using 100% cullet. In addition, it contributes to the reduction of greenhouse gas emissions and waste sent to landfills. These advantages have made glass recycling a central element of circular economy strategies aimed at minimising environmental impact while maintaining material value (Lebullenger et al., 2019).

However, despite its apparent simplicity, glass recycling is a technically complex process (Lebullenger and Mear, 2019). Labels, adhesives, metal closures, and organic residues from the glass's previous contents are among the many contaminants commonly found in glass that has been used for human consumption. In the initial stages of processing, a combination of mechanical and thermal methods must eliminate these contaminants. This is because these impurities may adversely affect both the melting behaviour of glass and the efficiency of sorting. The great variety of glass types and colours complicates the sorting process. Modern recycling plants increasingly rely on automated systems to separate glasses by colour and remove unwanted materials. These systems, such as optical sorters, are highly sensitive to the physical characteristics of the input material. Accurate sorting also depends on maintaining particle sizes within an optimal range, since excessively large or fine particles may interfere with sensor detection and separation. Insufficiently cleaned, poorly crushed, or unevenly shaped glass particles can result in considerable losses in sorting efficiency, ultimately diminishing the quality and output of the recycled product. The quality of the input material significantly influences both the sorting phase and subsequent processes, including melting and the fabrication of new glass products. When it comes to the melting stage, foaming, colour issues, and others might be caused by particles that have residue on

them or are irregularly shaped. It is possible that the manufacturing of glass will require more energy and the products will become less consistent if there are an excessive number of particles of varying sizes, poor flowability, and contamination. Because of this, ensuring that recycled glass is thoroughly prepared is an essential component in improving the efficiency of the entire recycling chain. To do this, it is necessary to ensure that the glass is sufficiently clean, that it is the appropriate size, and that it is physically homogeneous in terms of characteristics such as flow behaviour and density (Lebullenger et al., 2019).

Academic institutions have started looking into possible real-world solutions for these technical problems because they are of importance for both education and industry (see Chapter 2.4.5. Research and Development in Optical Sorting). The Department of Process Engineering at HAW Hamburg is currently working on building a small-scale optical glass sorting system to solve these problems and meet these needs. The goal of this platform is to create an academic environment that is both controlled and contained, similar to how things work in the real world. It will be used for both teaching and research purposes. The main goal of the practical part of this Bachelors Thesis is to make sure that a glass granulate is available that has been thoroughly prepared and consistently characterised. The success of this system depends a lot on whether or not this kind of granulate is available.

1.1. Task Description

The present bachelor thesis is part of a broader research effort in glass recycling at HAW Hamburg. The recycled glass granulates produced in this work will later be used in a subsequent master's project aimed at designing and testing a prototype optical sorting system. While the sorting process itself is not within the scope of this thesis, the preparatory steps required to provide a consistent and suitable bulk material are addressed here.

The primary task is to establish a reproducible procedure for generating standardised recycled glass granulate for laboratory-scale sorting. This includes the collection, cleaning, crushing, and characterization of clear and green post-consumer glass, with the aim of producing a target particle size range of 4–10 mm, considered optimal for mechanical and optical sorting systems. Furthermore, the granulate is prepared in a controlled colour composition of approximately 95% clear and 5% green glass to reflect a realistic but manageable sorting scenario.

In addition to particle size preparation, the thesis involves the evaluation of key material properties—such as particle size distribution, particle density, bulk density, tapped density, and porosity—using both manual and instrument-based methods, as well as flow behaviour. The compatibility of the material with common dosing technologies, such as vibrating chutes, is also examined.

By providing a well-characterised and standardised input material, this thesis creates a foundation for future research in optical glass sorting and supports practical education in sustainable process engineering.

Throughout this thesis, numerical values are written according to German notation, using commas as decimal separators.

2. Theoretical Background

This chapter provides the scientific and technical background necessary to understand the material and process aspects relevant to this thesis. It begins with a fundamental examination of glass as an engineering material, including its structural characteristics, classification, and manufacturing processes. These insights form the basis for evaluating the suitability of glass for recycling and interpreting its behaviour during reprocessing.

Building on this foundation, the chapter then focuses on the principles of glass recycling. It discusses the significance of recycling from both environmental and technical perspectives, followed by an overview of industrial process steps—from post-consumer waste to usable glass granulate—including collection and pre-cleaning, glass crushing (comminution), sizing, contaminant removal, and colour sorting. Special attention is given to the requirements that recycled glass material must fulfil in to ensure its compatibility with crushing-dependent particle size specifications, colour sorting systems and remelting processes. By combining material science fundamentals with recycling-specific considerations, this chapter aims to clarify the technical framework within which the experimental work of this thesis was developed.

2.1. Definition and Scientific Nature of Glass

Glass is scientifically defined as an amorphous, non-crystalline solid formed by the rapid cooling of a melt, which prevents the formation of a long-range ordered crystal lattice. Unlike crystalline materials, where atoms are arranged in periodic, repeating patterns, glass exhibits only short-range atomic order, resulting in a structurally disordered yet rigid solid. This structural disorder imparts many of glass's unique properties, including isotropy, optical transparency, and high chemical durability (Doremus, 1994; Varshneya, 1994). Owing to its nonequilibrium state, glass is often classified as a supercooled liquid, a term that reflects its thermodynamic metastability. The absence of long-range crystallinity leads to uniform properties in all directions (Schaeffer, 2020), which is essential in optical and technological applications. Moreover, the lack of grain boundaries—as typically found in polycrystalline materials—enhances its chemical resistance and minimises structural defects such as crack propagation and impurity diffusion (Abdelouas et al., 2019).

Figure 1 visualises the contrast between the periodic atomic structure of **crystalline silica** and the randomly connected network of **vitreous glass** (vitreous glass refers to glass in its amorphous, non-crystalline form, characterised by the absence of long-range order), emphasising the lack of long-range

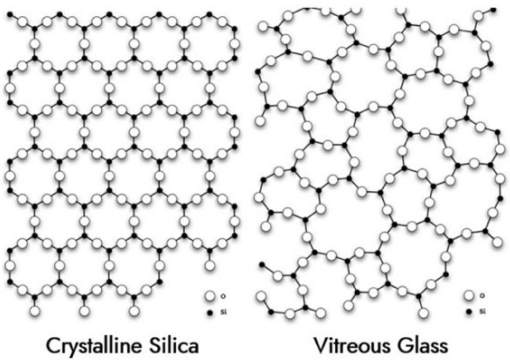

Figure 1: Structural comparison of crystalline silica and vitreous glass (Jones & Huff, 2018).

order in glasses (Doremus, 1994; Varshneya, 1994). Both are composed of SiO_2 units, but the glass structure forms upon rapid cooling of molten silica, resulting in an amorphous, non-crystalline network.

The formation of glass begins mostly with silica (SiO_2), which serves as the fundamental network-forming oxide in almost all commercial glass compositions. However, pure silica alone is rarely used efficiently to produce glassware or containers due to its extremely high melting point (~1700–1720 °C) and very high viscosity in the molten state, which make it difficult to process in standard industrial furnaces (Shelby, 2005; Varshneya, 1994). To overcome these limitations, silica is combined, for example, with sodium carbonate (Na_2CO_3)—a flux that lowers the melting temperature—and calcium carbonate ($CaCO_3$)—which improves chemical durability and thermal stability. Upon heating, these materials react to form sodium-calcium-silicate glass, the basis of soda-lime-silica glass, which accounts for over 90% of glass produced worldwide. This modified composition allows the melt to be formed at significantly lower temperatures (around 1400–1500 °C) and enables the production of glass with workable viscosity, improved shaping behaviour, and adequate resistance to chemical and thermal stress. The use of modifiers and stabilisers also makes it possible to fine-tune other properties, such as expansion coefficient, hardness, and refractive index—making soda-lime-silica glass highly versatile for a broad range of industrial and consumer applications (Doremus, 1994; Shelby, 2005; Varshneya, 1994).

From a thermodynamic perspective, glass does not possess a sharp melting point. Instead, it undergoes a glass transition—a gradual transformation from a rigid, brittle state to a viscous or rubber-like condition with increasing temperature. The glass transition temperature (T_g) occurs over a range and is highly dependent on the chemical composition and structural configuration of the glass-forming system (Abdelouas et al., 2019; Shelby, 2005). This behaviour clearly distinguishes glass, not only from crystalline solids but also from semicrystalline polymers. At the same time, the atomic-scale randomness of glass makes it thermodynamically metastable. Over long periods or under thermal treatment, glass can slowly begin to crystallise—a process known as devitrification—but this transformation is kinetically hindered under normal conditions (Shelby, 2005).

Understanding this structural and thermal behaviour is crucial for both industrial processing and recycling. The non-linear temperature dependence of viscosity makes glass difficult to form and remelt without defects. In recycling contexts, improper temperature control can lead to issues such as foaming, incomplete melting, or spontaneous crystallisation. In contrast to metals, which exhibit well-defined melting points and simple phase behaviours, glass requires tight thermal regulation during manufacturing and reuse (Doremus, 1994; Varshneya, 1994).

2.2. Classification of Glass Types

The recycling behaviour of glass requires a detailed understanding of its chemical composition and structural diversity. Glass is not a uniform material but encompasses a wide range of amorphous solids with distinct properties, manufacturing techniques, and end-use applications. These variations strongly influence glass's processability, melting behaviour, and above all, its compatibility with recycling systems. In practice, not all glass types can be recycled together, and some—such as lead crystal or borosilicate glass—pose challenges when mixed with mass-produced soda-lime silicate glass. Therefore, this section provides a structured classification of glass types, organised into three main groups and discussed with particular attention to their implications for post-consumer recycling and

remelting. A summary table outlining the typical composition and applications of each category will follow.

2.2.1. Composition-Based Glasses

One of the most common approaches to classify glass is by its chemical composition, particularly the primary component responsible for forming the amorphous network structure. These composition-based systems include a variety of oxide and non-oxide glass types, each characterised by different physical and chemical behaviours. Among the most industrially significant categories are silicate, borate, phosphate, and halide glasses, which differ not only in their structural formers but also in their thermal properties, processing conditions, and end-use applications.

1. Silicate Glasses

Silicate glasses are the most widely produced and technologically important class of glass materials. Their structure is primarily based on silicon dioxide (SiO_2), forming a three-dimensional network of SiO_4 tetrahedra interconnected via bridging oxygen atoms as shown in Figure 2 (Le Bourhis, 2008).

This continuous random network gives rise to high chemical durability and thermal stability (Schaeffer, 2020).

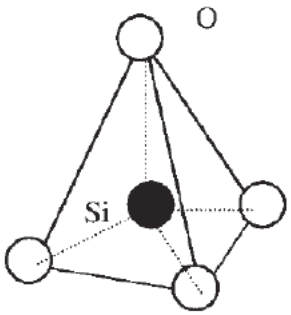

Figure 2: Tetrahedral Structure of Si and O (Le Bourhis, 2008).

Typical Composition

Silicate glasses are structurally modified through the addition of alkali and alkaline-earth oxides, such as Na_2O and CaO, which act as network modifiers. These break some of the Si–O–Si bonds, forming non-bridging oxygens (NBOs) and thereby reducing the viscosity and melting temperature of the glass. The most common type of silicate glass is soda-lime glass, with a typical composition of approximately 71.5–72 wt% SiO_2, 13–14 wt% Na_2O, and 10 wt%. Small amounts of Al_2O_3 and MgO may also be present. This composition provides a balance between processability and performance, making it suitable for large-scale industrial use (Le Bourhis, 2008; Le Losq et al., 2019).

Types and Applications

Soda-lime silicate glass is extensively used for container glass (e.g., bottles, jars) and flat glass (e.g., windows, facades). Good formability, optical clarity, and relatively low production costs support its widespread adoption. The float process has been the standard method for producing flat glass since the 1960s (Le Bourhis, 2008; Schaeffer, 2020). In packaging applications, particularly for beverage bottles, coloured silicate glasses are commonly used to improve light protection and aesthetic appearance. For example, as described in *Werkstoff Glas* (Schaeffer, 2020), brown glass for containers is produced by

the addition of iron oxides (Fe_2O_3), often in combination with sulphur compounds, resulting in shades ranging from yellow-brown to deep green depending on redox conditions. Another example is that Fe^{3+} and Fe^{2+} combinations are used to produce green and amber glass bottles, especially for beer and wine, to protect contents from UV degradation.

- Borosilicate glass, produced by adding B_2O_3, features enhanced thermal shock resistance and lower thermal expansion, making it suitable for laboratory glassware and cookware. Figure 3: Examples of laboratory glassware made from borosilicate glass. Source: SCHOTT AG (Schaeffer, 2020).

Figure 3: Examples of laboratory glassware made from borosilicate glass. Source: SCHOTT AG (Schaeffer, 2020).

- Lead crystal glass includes up to 35% PbO, increasing its optical brilliance and density. This type is mainly used for decorative items, but it is incompatible with container glass recycling due to its differing melting properties (Schaeffer, 2020).
- Aluminosilicate glass, which contains Al_2O_3, improves mechanical strength and thermal resistance, and is commonly used in optical applications and smartphone screens (Le Losq et al., 2019).

2. Borate Glasses

Borate glasses constitute a distinct category within the oxide glass family, characterised by the use of boron oxide (B_2O_3) as the primary network-forming component. While less common in mass production compared to silicate glasses, borate glasses are essential in technical applications that require unique thermal, optical, or dielectric properties (Schaeffer, 2020).

Typical Composition

Structurally, borate glasses consist of BO_3 triangles and BO_4 tetrahedra, with the ratio strongly influenced by network modifiers such as alkali oxides. This flexibility explains their variable viscosity, hardness, and chemical durability. In general, borate glasses soften at lower temperatures but show reduced resistance to aqueous environments, which limits their suitability for common packaging or container use (Feller, 2019; Le Bourhis, 2008).

Applications

Borate glasses are mainly used in specialised fields, such as sealing glasses for electronics and ceramics, thermal insulation materials, dielectric substrates, and as host matrices for rare-earth dopants in optical components (Feller, 2019). From a recycling perspective, their distinct composition and melting

behaviour make them incompatible with soda-lime silicate glass streams, restricting their large-scale reuse.

3. Phosphate Glasses

Phosphate glasses are oxide glasses in which phosphorus pentoxide (P_2O_5) functions as the main network former. Unlike silicate or borate systems, they are mainly used in niche technical applications due to their unique chemical and structural behaviours (Schaeffer, 2020).

Typical Composition

Their structure is based on PO_4 tetrahedra forming either chain-like or moderately crosslinked networks. Modifiers such as Al_2O_3 improve thermal stability, while CaO contributes to bioresorbability in biomedical applications. These glasses generally exhibit lower durability in aqueous environments, which can be advantageous for controlled ion release but unsuitable for packaging or container applications (Munoz et al., 2019).

Applications

Phosphate glasses are valued for their bioactivity and optical properties. Typical uses include bone regeneration and drug delivery systems, low-temperature sealing glasses, and rare-earth-doped laser host materials. Due to their high solubility and different melting characteristics, they cannot be recycled together with soda-lime glass and therefore remain outside large-scale recycling processes. Although they are not suitable for conventional packaging or container applications due to lower chemical durability, phosphate glasses offer significant advantages in highly controlled, functional environments, especially in biomedicine and laser technologies. (Munoz et al., 2019; Schaeffer, 2020).

4. Halide Glasses

Halide glasses are non-oxide systems in which halogen anions, primarily fluorides but also chlorides or bromides, act as key constituents. They differ fundamentally from oxide glasses due to their ionic bonding and are mainly relevant for optical technologies (Clare et al., 2019).

Typical Composition

The most important family is fluoride-based glasses, particularly ZBLAN (ZrF_4–BaF_2–LaF_3–AlF_3–NaF), which offers wide infrared transmission up to 7 µm. While they exhibit unique optical performance, they are also prone to devitrification and sensitive to moisture, requiring highly controlled production environments (Clare et al., 2019).

Applications

Halide glasses are applied in infrared fibre optics for medical imaging and sensing, rare-earth-doped fibre lasers, and specialised nonlinear optical systems. Despite their technical importance, their distinct composition and instability make them incompatible with soda-lime recycling, and they are therefore excluded from conventional post-consumer recycling streams (Clare et al., 2019).

2.2.2. Natural Glass

Natural glasses are formed by high-temperature geological events such as volcanic eruptions, lightning strikes, or meteorite impacts. They share the amorphous structure of synthetic glasses but differ in origin

and composition (Cicconi & Neuville, 2019; Le Bourhis, 2008; Schaeffer, 2020). Typical examples include:

1. **Obsidian –** volcanic glass with high silica content, historically used for tools (Cicconi & Neuville, 2019).
2. **Tektites** – impact glasses ejected during meteorite collisions, relevant in planetary science (Cicconi & Neuville, 2019).
3. **Lunar Glass** – impact-generated glasses on the Moon, important for extraterrestrial geology (Le Bourhis, 2008).

While scientifically valuable, natural glasses play no role in large-scale industrial recycling and are only discussed here for completeness.

2.2.3. Functional Glasses

1. Metallic Glasses

Metallic glasses (amorphous metals) are multicomponent alloys produced by rapid quenching. (Pelletier & Qiao, 2019).

Typical Composition

Systems such as Zr–Ti–Cu–Ni–Be or Fe–B–Si are examples of typical compositions (Pelletier & Qiao, 2019).

Applications

High-strength components, MEMS, biomedical devices, and magnetic materials. Their metallic nature makes them irrelevant for conventional glass recycling (Le Bourhis, 2008; Pelletier & Qiao, 2019).

2. Bioactive Glasses

Bioactive glasses are silica-based compositions (e.g., Bioglass® 45S5 with SiO_2–Na_2O–CaO–P_2O_5) designed to bond with tissue (Hupa et al., 2019).

Typical Composition

Relatively low silica with high Na_2O and CaO content (Hupa et al., 2019).

Applications

Applications include bone regeneration, dentistry, and implant coatings. Due to their niche production and special chemistry, they are excluded from recycling streams for container glass (Hupa et al., 2019).

2.2.4. Summary of Classification and Composition of Glass Types

To further clarify the chemical differences among glass categories, Table 1: Typical Composition and Application of Selected Glass Types provides a summary of the typical compositions, main network formers, and primary application areas of the most relevant glass types. This structured comparison serves to contextualise why certain glass types behave differently in processing and recycling, and helps identify which categories are compatible with standard manufacturing and remelting systems.

Table 1: Typical Composition and Application of Selected Glass Types (source: compiled from Werkstoff Glas: Alter Werkstoff mit Großer Zukunft (Schaeffer, 2020), Springer Handbook of Glass (2019) , and Glass: Mechanics and Technology (Le Bourhis, 2008)).

Glass Type	Main Network Former(s)	Typical Composition (wt%)	Notes / Applications
Soda-lime Silicate Glass	SiO_2	71.5% SiO_2, 13% Na_2O, 10% CaO	Containers, flat glass, windows
Borosilicate Glass	$SiO_2 + B_2O_3$	≈70% SiO_2, 10–13% B_2O_3, modifiers	Lab glassware, cookware, chemical resistance
Borate Glass	B_2O_3	Na_2O–B_2O_3 or Li_2O–B_2O_3	Sealing glasses, optical materials, scientific uses
Phosphate Glass	P_2O_5	45% SiO_2, 24.5% Na_2O, 24.5% CaO, 6% P_2O_5	Bone regeneration, bioresorbable implants
Halide Glass (ZBLAN)	ZrF_4 (fluoride-based)	ZrF_4, BaF_2, LaF_3, AlF_3, NaF	IR optics, laser systems, thermal imaging
Obsidian	SiO_2	74.6% SiO_2, 12.75% Al_2O_3, trace Fe_2O_3, MgO	Prehistoric tools, geological research
Tektite (e.g., Australite)	SiO_2	76.1% SiO_2, 13.1% Al_2O_3, trace Fe_2O_3, MgO	Planetary science, impact studies
Lunar Glass	SiO_2	54.5% SiO_2, 23% MgO, 21.4% Fe_2O_3	Lunar geology, extraterrestrial materials
Metallic Glass (e.g., Vitreloy)	Metal atoms (e.g., Zr, Ti)	Zr–Ti–Cu–Ni–Be (multicomponent alloy)	High strength, corrosion resistance, MEMS, biomedical
Bioactive Glass (Bioglass® 45S5)	$SiO_2 + P_2O_5$	45% SiO_2, 24.5% Na_2O, 24.5% CaO, 6% P_2O_5	Bioactive implants, bone repair, dental use

Colouring ions are introduced in very small quantities but significantly affect the optical transmission of glass. Table 2 summarises the common colouring ions used in glassmaking, including their oxidation states, coordination geometries, and the characteristic colours they produce. The choice of colouring agents is also relevant in the context of recycling, as mixed-colour cullet may require optical sorting systems that distinguish between shades.

Table 2: Colouring Ions in Glass and Their Optical Effects (adapted from Werkstoff Glas: Alter Werkstoff Mit Großer Zukunft (Schaeffer, 2020)).

Ion	Oxidation State	Coordinate Geometry	Colour in Glass	Usually used for
Co^{2+}	2+	Octahedral	Deep blue	Decorative glass and optical filters
Cr^{3+}	3+	Octahedral	Green	Container glass, optical uses
Cr^{6+}	6+	Tetrahedral	Yellow	Signal glass, special color effects
Cu^{2+}	2+	Octahedral	Blue-green	Art glass, tableware
Fe^{2+}	2+	Octahedral	Pale blue	Historic glassware
Fe^{3+}	3+	Octahedral	Yellow to brown	Container glass coloration
Mn^{2+}	2+	Octahedral	Pink	Color correction glass
Mn^{3+}	3+	Octahedral	Violet	Specialty colored glass
Ni^{2+}	2+	Octahedral	Brown	Neutral gray glass
U^{6+}	6+	Various	Yellow-green fluorescence	Fluorescent and uranium glass

2.3. Glass Manufacture

The production of glass is a multi-stage process that transforms raw materials into a homogeneous, solid, and often optically clear product. While the foundational principles remain consistent, specific practices and technological details can vary based on the type of glass being produced and the intended application.

2.3.1. Raw Material and Batching

Raw materials in glass production are chosen based on the required composition and characteristics. Network formers like SiO_2 are derived from quartz sand, whereas Na_2CO_3 functions as a flux, and $CaCO_3$ or dolomite contributes to the network's stability. Additional oxides, colouring agents, or fining additives may be used depending on the type of glass (Schaeffer, 2020; Shelby, 2005).

Recycled glass (cullet) plays a vital function by lowering melting temperature and energy requirements. Cullet can constitute up to 95% in green glass, 60–80% in brown glass, and 50–70% in clear glass, but flat glass manufacturing predominantly depends on internal cullet due to purity standards. In addition to its ecological benefits, cullet enhances melting efficiency and promotes uniformity, hence directly affecting product quality (Le Bourhis, 2008; Schaeffer, 2020).

2.3.2. Melting and Refining

The batched mixture is introduced into large melting furnaces operating at temperatures exceeding 1400°C. Early heating stages initiate solid-state reactions and decomposition of carbonates, releasing gases like CO_2 (Shelby, 2005). As temperatures increase, eutectic melts form between the components, promoting dissolution of more refractory materials such as quartz. The outcome is a homogeneous viscous melt with well-formed silicate networks (Le Bourhis, 2008).

Melting furnaces vary depending on the glass type. (Schaeffer, 2020) The most common designs include:

- **Cross-fired regenerative furnaces**: high capacity (up to 1000 t/day), typical for flat glass production, with alternating burners and heat recovery.
- **End-fired regenerative furnaces**: more compact, used mainly for container glass (up to 400 t/day).
- **Electric furnaces**: offering precise thermal control, mainly for speciality glass.

A schematic of a cross-fired regenerative furnace is shown in Figure 4, illustrating the main zones for batch charging, melting, refining, and heat recovery. After melting, the glass must be refined to remove entrapped gases that compromise clarity. This is achieved by maintaining high temperature to reduce viscosity and by adding fining agents such as Na_2SO_4 or As_2O_3 to promote bubble removal (Le Bourhis, 2008; Shelby, 2005).

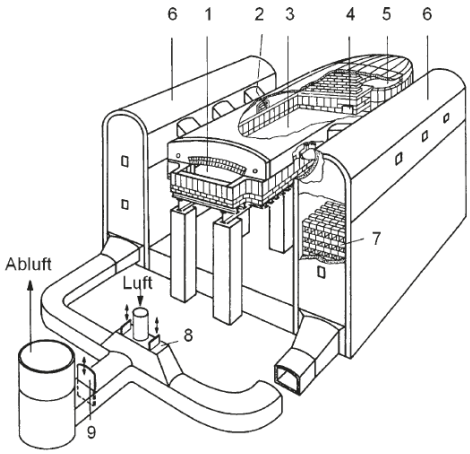

Figure 4: Cross-fired regenerative glass melting furnace. (1) Batch charger, (2) burners, (3) melting tank, (4) throat (passage), (5) working end (refining zone), (6) regenerators, (7) checkerwork chambers, (8) reversing unit, and (9) chimney damper. Image credit: W. Trier, Glass Melting Furnaces, Springer Verlag, 1984 (Schaeffer, 2020).

Thermal Behaviour and Viscosity Characteristics

The melting and working behaviour of glass is strongly influenced by its viscosity, which changes with temperature. Different types of technical glasses—such as soda-lime, borosilicate, and fused silica—

exhibit distinct softening points and transformation temperatures. Table 3 summarises typical viscosity-related temperature points for selected glasses, adapted from *Glasbau* (Schneider et al., 2016), based on data from Pfaender (1997), Öksoy et al. (1994), and SCHOTT AG.

Table 3: Characteristic Viscosity-Dependent Temperatures for Technical Glasses (Adapted from *Glasbau* (Schneider et al., 2016)).

Viscosity [dPas]	Description	Soda-Lime Glass [°C]	Borosilicate Glass [°C]	Fused Silica [°C]
10^4	Working temperature *(T_t)*	1030	1260	2100
$10^{7,6}$	Softening temperature *(T_{so})*	725	825	1730
10^{13}	Upper annealing temperature *(T_a)*	550	560	1180
$10^{13,3}$	Glass transition temperature *(Tg)*	530	525	1140
$10^{14,5}$	Lower annealing temperature *(T_{st})*	506	518	1075

Soda-lime glass, with relatively low working and softening temperatures, can be formed efficiently in large-scale production. Borosilicate glass requires higher processing temperatures, while fused silica demands extremely high thermal input, explaining its limited industrial use despite superior material properties.

Energy Considerations

Melting consumes the most energy in the glassmaking process. The theoretical energy demand without cullet is approximately 2.6 GJ/t. Practical values in regenerative furnaces reach ~2.9 GJ/t. Using cullet reduces this demand significantly by eliminating carbonate decomposition and lowering the melting temperature, thus improving both energy efficiency and furnace lifetime (Schaeffer, 2020).

2.3.3. Homogenisation and Conditioning

Even after fining, compositional variations can persist. (Shelby, 2005) describes homogenisation processes that rely on convective flow, diffusion, and sometimes mechanical stirring to eliminate streaks or striae. Conditioning zones in the furnace maintain a stable temperature and viscosity prior to forming. The book *Werkstoff Glas* highlights methods such as stirring paddles and bubblers, which help stabilise the melt. This step ensures a uniform melt quality, which is equally critical when cullet is incorporated, as impurities or compositional variations could otherwise lead to defects (Martens & Goldmann, 2016; Schaeffer, 2020).

2.3.4. Forming Techniques

Glass is formed within a viscosity range of 10^3–10^8 Pa·s, employing techniques tailored to the specific product type. The float technique, wherein molten glass disperses over molten tin, predominates flat

glass manufacturing owing to its capacity to produce uniform sheets. Pressing is utilised for dinnerware and jars, whereas blow-blow and press-blow techniques are fundamental to container manufacturing, guaranteeing accurate wall thickness. The fusion draw process is employed for specialist products like ultra-thin display glass, facilitating sheet production without contact with solid moulds (Le Bourhis, 2008; Schaeffer, 2020).

2.3.5. Annealing

After forming, glass is cooled in a controlled manner to release internal stresses. Rapid cooling would otherwise cause cracking or breakage. Annealing takes place in lehr kilns, typically very long for flat glass (≈150 m) or in staged conveyor kilns for container glass. The process occurs just below the glass transition temperature, enabling molecular relaxation without deformation (Le Bourhis, 2008; Schaeffer, 2020; Shelby, 2005).

2.3.6. Post-Processing and Finishing

Many products undergo further treatment to enhance performance or aesthetics. Processes include:

- Tempering: Thermal or chemical strengthening to increase mechanical resistance,
- Polishing/Etching: For optical properties or decorative effects,
- Surface Coatings: Such as anti-reflective layers or photocatalytic self-cleaning films,
- Quality Control: Visual inspection and optical scanning for dimensional and structural defects (Le Bourhis, 2008).

2.3.7. Specialised Melting Methods

According to *Introduction to Glass Science and Technology*, some glass types require unique melting environments due to volatility or reactivity (Shelby, 2005):

- Chalcogenide Glasses: Melted in sealed ampoules to prevent oxidation.
- Halide Glasses: Require reactive atmospheres to preserve halide content.
- Containerless Melting: Techniques like aerodynamic levitation allow ultra-clean melts for research purposes.

2.3.8. Conclusion

Glass manufacturing involves a sequence of precisely controlled steps: from raw material preparation to melting, refining, shaping, annealing, and finishing. The effectiveness of each stage directly influences product quality and energy efficiency. While foundational techniques remain similar across glass types, innovations in furnace design, forming, and post-processing continue to expand the scope of glass applications across modern industry.

2.4. Glass Recycling

Glass recycling plays a pivotal role in both environmental sustainability and industrial process optimisation. As one of the few materials that can be recycled indefinitely without loss of quality, glass occupies a unique position in circular economy strategies. Beyond its ecological benefits, the use of recycled glass—or cullet—provides significant process-related advantages in glass manufacturing.

From a process engineering perspective, incorporating cullet into the glass batch reduces the melting temperature by approximately 100 to 200 °C compared to raw materials, which in turn lowers energy consumption and operating expenses. Studies show that replacing virgin materials with 100% cullet can reduce CO_2 emissions by up to 670 kg per tonne of glass produced, while also saving roughly 1,2 tonnes of raw materials, including silica sand, soda ash, and limestone (*FEVE-Brochure-Recycling-Why-Glass-Always-Has-a-Happy-CO2-Ending*, n.d.). This energy and material efficiency contributes not only to climate goals but also to furnace longevity, as cullet melts more uniformly and gently, reducing wear on refractory materials (Doremus, 1994; Shelby, 2005).

Glass is also chemically inert and non-toxic, making it particularly suitable for reuse in sensitive applications such as food and beverage packaging or pharmaceutical containers. Its structural stability ensures that no harmful substances leach into the contents, even after repeated recycling cycles (Abdelouas et al., 2019).

Figure 5: Source-separated glass recycling bins in Europe (UK, France, Germany), used for voluntary collection by colour. Source: Springer Handbook of Glass (Lebullenger et al., 2019).

Strict regulatory targets further underscore the significance of glass recycling in Europe. The EU Packaging Waste Directive (European Commission, 2018) mandates that at least 75% of all glass packaging must be recycled by 2030. Countries like Germany already surpass these targets due to efficient infrastructure, including deposit-return systems (*Pfandsysteme*) and colour-sorted collection shown in Figure 5: Source-separated glass recycling bins in Europe (UK, France, Germany), used for voluntary collection by colour. Source: Springer Handbook of Glass(Lebullenger et al., 2019).

However, achieving high-quality recycled output remains dependent on input purity. The presence of ceramics, heat-resistant glass, or organic residues can compromise melting behaviour and product integrity. Therefore, glass recycling must be viewed not only as an environmental imperative but also as a technically demanding process. Achieving high yields and maintaining product quality require careful control over cullet properties, contamination levels, and preparation methods—factors which are directly addressed in the experimental and theoretical framework of this thesis.

As glass is chemically and thermally stable—primarily due to the strong Si–O bonds within its silicate structure—it cannot be reconverted into its original raw materials through chemical decomposition. Therefore, unlike plastics, glass recycling is only feasible through material reuse, which maintain the structure of the original material. This feat is typically achieved by re-melting cullet (waste glass shards) with virgin raw materials in glass furnaces (Martens & Goldmann, 2016).

The durability of silicate-based glass makes it an ideal candidate for repeated recycling without degradation in quality. However, it also means that only a specific type of recycling process is practical: one that preserves the material structure. The high temperatures involved in glass melting and the strong resistance of silicate matrices to breakdown or leaching limit alternative recovery routes.

Due to these factors, the glass recycling process is divided into three fundamental stages:

1. Destruction of the used form and production of suitable particle sizes.
2. Removal of foreign materials and contaminants.
3. Remelting and shaping into new glass products.

This section provides an in-depth overview of the technical, material, and process-based aspects of glass recycling, focusing on different glass types, required purity levels, processing technologies, and challenges in implementation (Martens & Goldmann, 2016).

2.4.1. Material Characteristics of Glass and Implications for Recycling

Glass materials are primarily composed of silicates, supplemented with oxides (e.g., Al_2O_3, MgO, ZrO_2) or other compounds such as carbides (SiC) and nitrides (BN, AlN). These materials are known for their high thermal and chemical stability, primarily resulting from the stability of the SiO_4 tetrahedral structures in silicate networks (Martens & Goldmann, 2016).

In the production of glass, the raw materials typically include:

- Aluminosilicates (e.g., clay, kaolin),
- Quartz sand (SiO_2),
- Carbonate-based materials such as limestone ($CaCO_3$), dolomite ($CaCO_3 \cdot MgCO_3$), and soda (Na_2CO_3).

Due to the highly stable nature of silicate glass networks formed during melting, reversing them into their original raw components is neither technically feasible nor economically justified. Therefore, unlike some polymers or metals, glass cannot undergo chemical or feedstock recycling. Instead, it is recycled exclusively through material reuse by remelting the glass without altering its chemical structure (Martens & Goldmann, 2016).

Importantly, silicate glass melts have a high solubility for many other metal oxides, which allows them to incorporate a wide range of additives (e.g., colourants) and contaminants. This property is advantageous in waste management applications where certain toxic components can be safely immobilised within the glass matrix. The implication of this material stability is that glass recycling always involves preserving the glassy structure, either through remelting or direct integration of cullet into new products. Therefore, precise control over composition and particle size is essential in all stages of the recycling process (Martens & Goldmann, 2016).

2.4.2. The Recyclability of Glasses

From a recycling perspective, not all glass types are equally suitable for reuse. While glass may be broadly classified based on its chemical composition and structure (as discussed in Chapter 2.2), these classifications have direct implications for recyclability in post-consumer applications.

The German glass industry, for instance, produced approximately 3,01 million tonnes of container glass and 1,69 million tonnes of flat glass in 2006, compared to only 0,36 million tonnes of speciality glass. Due to their high production volume and relatively uniform composition, container glass and flat glass are the main focus of large-scale industrial recycling efforts. These glasses, primarily based on alkali-alkaline earth silicate systems, are chemically compatible and processable in shared melting systems (Martens & Goldmann, 2016).

According to (Lebullenger et al., 2019; Martens & Goldmann, 2016), speciality glasses—such as borosilicate laboratory glassware, lead crystal, cathode ray tube (CRT) glass, and coloured or coated display glasses—pose significant challenges for recycling:

- Borosilicate glass, due to its high thermal and chemical resistance, melts at different temperatures and is incompatible with standard soda-lime furnaces.
- Lead-containing glasses such as CRT funnels or decorative crystal must be handled with care due to the environmental risks of PbO.
- Optically coated or coloured glasses may interfere with glass colouration or transparency in recycled products.
- Glasses from electronics or automotive sources often contain adhesives, coatings, or composite layers that require advanced separation steps.

Figure 6 illustrates common examples of acceptable and non-acceptable items for glass recycling.

Figure 6: Accepted and rejected items in container glass recycling. Source: Springer Handbook of Glass (Lebullenger et al., 2019).

The recyclability of glass is therefore determined by factors such as (Lebullenger et al., 2019; Martens & Goldmann, 2016):

- Volume and consistency of the waste stream (mass-produced vs. niche use),
- Chemical compatibility with standard glass recipes,
- Presence of contaminants or hazardous materials,
- Economic feasibility of collection, sorting, and reprocessing.

Consequently, modern glass recycling infrastructure prioritises mass-market soda-lime glasses (e.g., bottles, jars, windowpanes) over technically demanding speciality glasses, which are often directed to niche secondary uses or excluded from recycling altogether (Martens & Goldmann, 2016).

2.4.3. The Glass Melting Process and Use of Cullet

The melting process lies at the heart of glass production and recycling. In industrial practice, glass is produced by melting a batch mixture of raw materials and cullet to form a homogeneous, bubble-free glass melt. The process operates continuously in large, gas-heated tank furnaces (*Glasschmelzwannen*),

which are lined with refractory bricks and reach temperatures of up to 1600 °C (Martens & Goldmann, 2016).

Raw Materials and Batch Composition

As also mentioned before, primary raw materials used in soda-lime glass production include:

- Quartz sand (SiO_2) – the primary glass former,
- Soda ash (Na_2CO_3) – reduces the melting temperature,
- Limestone and dolomite ($CaCO_3$ and $CaMg(CO_3)_2$) – provide CaO and MgO for chemical durability,
- Feldspar or alumina sources – to supply Al_2O_3 (Martens & Goldmann, 2016).

In addition, glass cullet from in-house production or external post-consumer sources is added to the batch. In-house cullet typically comprises 10–20% of the total batch, while post-consumer cullet can account for 20–90%, depending on availability and product requirements (Martens & Goldmann, 2016).

Cullet contributes significantly to the efficiency of the melting process:

- Reduction in primary raw materials,
- It melts more quickly than raw materials, reducing overall melting time,
- Each percent of cullet addition can lower energy consumption by approximately 0,25–0,3%,
- It enhances homogeneity by promoting early melt formation (*Scherbenschmelze*), and
- It supports gas release from decomposing carbonates and hydrates, aiding bubble removal and mixing (Lebullenger et al., 2019; Martens & Goldmann, 2016).

However, these benefits are highly dependent on cullet quality. The glass industry distinguishes between:

- **In-house cullet (*Eigenscherben*)**: clean, compositionally known,
- **External cullet (*Fremdscherben* or *Altglasscherben*)**: varied in type and often contaminated (Martens & Goldmann, 2016).

Melting Stages

The glass melting process by recycling process is not much a different as explained in Chapter 2.3.2. *Recyclingtechnik* by (Martens & Goldmann, 2016) comprises several distinct phases:

1. **Charging and Heating (1100-1500°C)**

   The batch is fed onto a hot melt surface. Silicate formation occurs first, followed by cullet melting and final dissolution of residual quartz.

2. **Homogenisation (1600 °C)**

   Gas bubbles from carbonates and hydrates rise and mix with the melt. Additional stirring or gas injection may be used to achieve chemical and thermal uniformity.

3. **Fining (1600 °C)**

   This step removes residual gas bubbles. Fining agents such as Na_2SO_4 (which decomposes to release SO_2 and O_2 at >1,200 °C) or As_2O_3 are added to promote bubble migration to the surface.

4. **Conditioning (1200–900 °C),**

   The melt is cooled to forming temperature (ca. 900–1200 °C), ready for shaping.

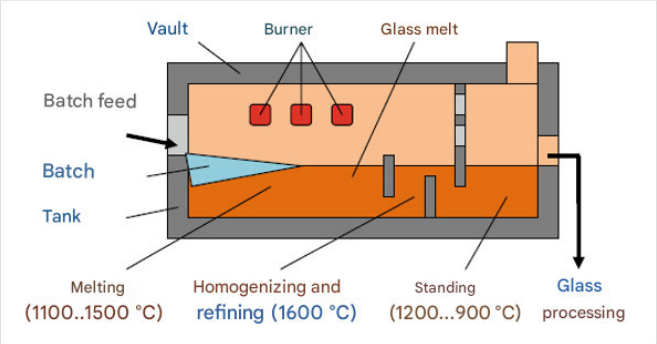

Figure 7: Glass melting tank and processing zones (translated from Martens & Goldmann, 2016).

Figure 7 is illustrating the stages of melting, homogenisation, and conditioning with their respective temperature ranges.

In summary, the use of cullet in the glass melting process is not only economically advantageous but also technologically essential for energy savings, emissions reduction, and improved melt quality. However, these benefits can only be realized when cullet meets **stringent purity and particle size requirements**—setting the stage for advanced preprocessing and sorting techniques, discussed in the next section.

2.4.4. Container Glass Recycling: Processing and Sorting

Container glass—primarily used for bottles and jars—is the most recycled type of glass in Europe. Its relatively consistent composition (soda-lime silicate glass), large production volumes, and centralized return systems make it highly suitable for industrial-scale recycling. In Germany, approximately **70,6%** of collected container glass originates from beverage bottles, which have a high return rate, with the remainder being pharmaceutical, cosmetic, and food packaging glass. To be reused in container glass production, post-consumer cullet must meet strict quality standards, especially regarding colour, chemical purity, and particle size distribution (Martens & Goldmann, 2016).

Influence of Contaminants and Impurities

Post-consumer cullet is often contaminated with:

1. Incorrect glass colours – affects final glass colour quality and requires precise colour sorting (Lebullenger et al., 2019; Martens & Goldmann, 2016).
2. Ceramics, stones, and porcelain (KSP) – poorly soluble in melts; they can form unmelted inclusions, causing defects in products (Martens & Goldmann, 2016).
3. Metals – Tin, lead, and copper sink to the furnace bottom and accelerate corrosion; aluminium and zinc fully dissolve and can interfere chemically; iron partially oxidizes (Lebullenger et al., 2019; Martens & Goldmann, 2016).
4. Organics – Mostly burn off, but can affect redox conditions, impacting melt colouration and fining (Lebullenger et al., 2019; Martens & Goldmann, 2016).

The effectiveness of cullet usage is highly dependent on its purity. Natural raw materials, particularly quartz sand, are selected based on low Fe_2O_3 content (max. 0.1% in flat glass). Table 4 shows the purity requirements and impurity limits of quartz sand used in glassmaking.

Table 4: Typical impurity limits in quartz sand (Types A and B), indicating threshold values for SiO_2 purity and trace oxides (Adapted from Recyclingtechnik (Martens & Goldmann, 2016)).

Constituent	Type A Quartz Sand (%)	Type B Quartz Sand (%)
SiO_2	99,65	~95
Fe_2O_3	0,025	max. 0,004
Al_2O_3	0,20	1,5
CaO + MgO	0,01	max. 1,5
$Na_2O + K_2O$	0,02	–
Loss on Ignition	0,10	max. 1,5

To ensure high-quality output, the German Glass Recycling and Waste Prevention Association (GGAmbH) and the Federal Association for Secondary Raw Materials and Waste Management (BVSE) have defined specifications for melt-ready container glass cullet. A summary of key parameters is provided below in Table 5: Quality criteria for container glass cullet by GGAmbH and (Martens & Goldmann, 2016).

Table 5: Quality criteria for container glass cullet by GGAmbH and BVSE (Based on Recyclingtechnik (Martens & Goldmann, 2016)).

Parameter	Clear Glass	Green Glass	Brown Glass
Minimum Purity	97%	97%	97%
Max Foreign Matter	1%	1%	1%
Max Wrong Glass Type	2%	2%	2%
Max Colour Deviation	3%	15%	8%

The following issues with glass quality could result from cullet contaminations and impurities:

- Inclusions or colour changes,
- Problems with glass melting due to foaming or insufficient heat transfer,
- Reduced glass furnace lifespan due to the metal melts in the cullet being drilled downward (Lebullenger et al., 2019).

Processing Steps

1. **Manual Pre-Sorting (*Handausleseband*)**
   The recycling process begins with manual pre-sorting on a conveyor belt to remove coarse contaminants such as large metal parts, stones, ceramics, and other non-glass debris. This stage ensures that oversized or potentially damaging materials are excluded before mechanical processing. The remaining material is then directed to a primary sieving stage (Martens & Goldmann, 2016).

2. **Initial Sieving *(1. Siebklassierung*)**

The material is classified into two size fractions using a sieving unit. Particles smaller than 45 mm proceed directly to magnetic separation, while those larger than 45 mm are sent for further manual inspection followed by comminution. This split ensures that only oversized fragments undergo energy-intensive crushing, optimising processing efficiency (Martens & Goldmann, 2016).

3. **Manual Re-sorting for >45 mm Fraction**

Larger particles are subjected to another manual inspection to remove any remaining contaminants before mechanical size reduction. This step protects the crushing machinery and improves downstream process reliability (Martens & Goldmann, 2016).

4. **Impact Mills (*Prallmühle*)**

Particles larger than 45 mm are reduced in size using an impact mill *(Prallmühle*). It is stated in *Recyclingtechnik* that the essential step in the processing line is crushing the collected glass using an impact mill. This equipment breaks down the container glass into grain sizes of approximately 5 to 60 mm, which are accordingly optimal for all subsequent sorting steps. This particle size ensures that materials can be efficiently processed by mechanical, magnetic, and sensor-based systems (Martens & Goldmann, 2016).

Impact mills operate with a high-speed rotor that accelerates the glass fragments and propels them against stationary impact plates, causing breakage by repeated collisions between particles and machine surfaces. This principle allows for selective fragmentation of brittle materials such as glass and ceramics, while more elastic contaminants tend to remain as oversize fractions.

The construction and working principle of an impact mill are illustrated in Figure 8. Compared to jaw or hammer crushers, impact mills generate a narrower size distribution and more angular particles, which is advantageous for downstream optical sorting (Martens & Goldmann, 2016; Thomé-Kozmiensky & Hoffmann, 2010).

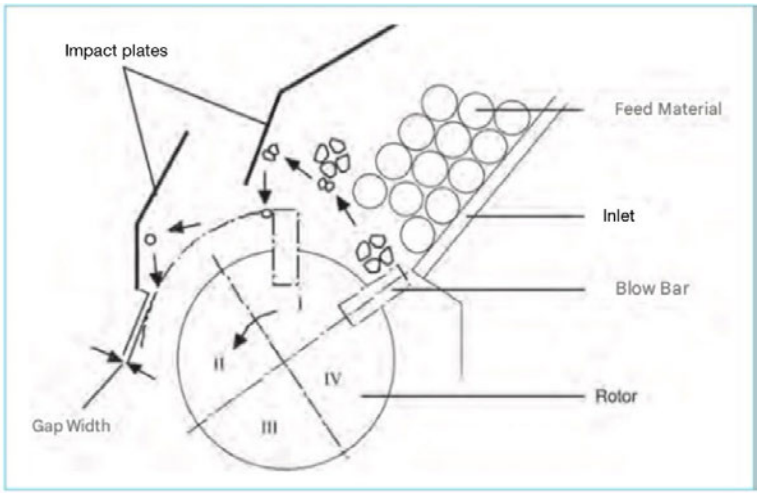

Figure 8: Principle sketch of an impact mill (Prallmühle), showing feed inlet, rotor with blow bars, impact plates, and discharge gap (translated from Mechanische Aufbereitung von Abfällen (Thomé-Kozmiensky & Hoffmann, 2010)).

The target particle range of 5–60 mm is particularly relevant because sensor-based sorting technologies perform most efficiently on medium fractions. Commercial systems such as the Sesotec K9 operate from particle sizes of about 2 mm, while others like the Suibo AC1200 are optimised for ranges of 8–60 mm, and Binder+Co's CLARITY systems also specify similar

operating windows (Binder+Co AG, 2021; Sesotec GmbH, 2023; Suibo Machinery, 2022). These specifications underline why impact mills are favoured in practice: they reliably deliver cullet within the required size range for high-precision optical colour and contaminant separation.

Despite their advantages—high throughput, consistent particle geometry, and satisfactory compatibility with optical sorting—impact mills also have limitations. They tend to generate fine fractions below 4 mm, which are difficult to detect in optical sorters and are often rejected, lowering the effective yield. Additional sieving stages are therefore required to remove undersized particles and maintain cullet quality (Thomé-Kozmiensky & Hoffmann, 2010). Nevertheless, their efficiency and ability to handle large volumes explain why impact mills remain the preferred technology in industrial container glass recycling across Europe (Lebullenger et al., 2019; Martens & Goldmann, 2016).

5. **First Magnetic Separation**

   Ferrous metals are removed using magnetic separators placed along both processing lines: before and after crushing. This ensures that metal contaminants are extracted early in the process to avoid interference with further processing and to prevent furnace damage during remelting (Martens & Goldmann, 2016).

6. **Pre-Sorting Technology**

   At this stage, sophisticated sensor-based systems begin to classify the cullet. KSP detectors (for ceramics, stones, and porcelain), sensors for fine metal particles, and colour-based rejectors identify and separate non-glass or miscoloured fragments. An air classifier (*Windsichter*) may also be used here to remove lightweight contaminants such as paper, foil, and plastic (Martens & Goldmann, 2016).

7. **Second Magnetic Separation (if needed)**

   An additional magnetic separation step may be employed for crushed material to ensure any residual ferrous metals are removed. This is particularly useful when the crushing process exposes previously embedded metal fragments (Martens & Goldmann, 2016).

8. **Second Sieving and Grain Classification**

   The material is sieved again to produce narrow particle size ranges. Particles smaller than 4 mm are usually discarded due to poor detectability in optical sorting systems. This refined classification is critical for ensuring accuracy in downstream sensor-based systems. The particle size of the cullet undergoes sieving to divide the crushed glass into particle fractions:

   - <4 mm: max 5%
   - 4–16 mm: 30%
   - 16–60 mm: 50%
   - Max size: 80 mm

   This controlled size range is necessary for consistent performance in sensor-based and mechanical separation systems (Martens & Goldmann, 2016).

9. Second Sensor Sorting

Each particle size class undergoes a second round of sorting. These sensor systems include optical transparency detection, multicolour laser scanners, and advanced reflectivity sensors. In cases where conventional optical methods fail (e.g., glass-ceramic, lead crystal), X-ray or spectral analysis may be used to identify and remove problematic materials (Martens & Goldmann, 2016).

10. Third Magnetic Separation

As a final control step, magnetic separation is applied again to remove any last traces of ferrous contaminants. This ensures high purity of the final cullet output (Martens & Goldmann, 2016).

11. Final Product: Refined Cullet Granulate

The final product is a clean, homogeneously sized glass cullet with a typical purity of up to 99.5%. For clear glass, colour purity must reach at least 99.7%, often requiring the addition of high-quality primary raw materials. The refined cullet is ready for remelting in container glass production (Martens & Goldmann, 2016).

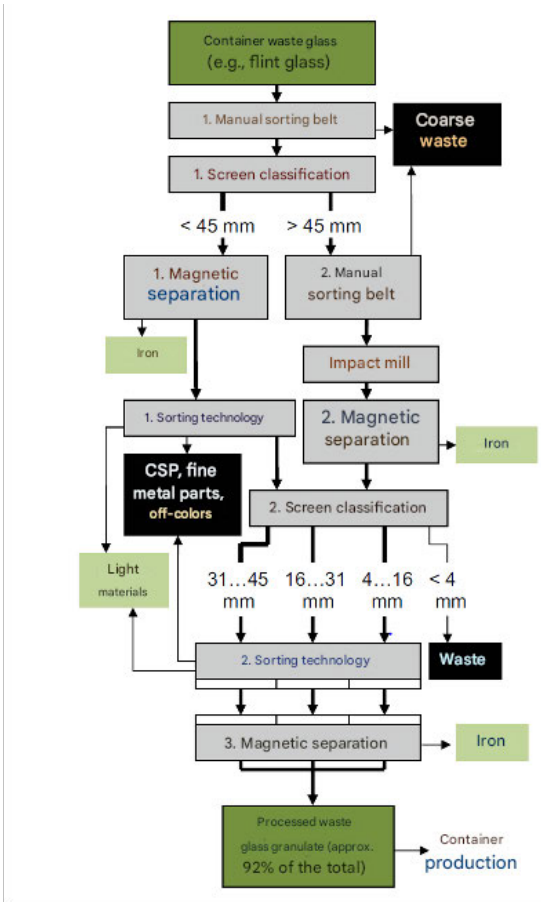

Figure 9: Process flow for container glass cullet treatment, showing sorting, crushing, magnetic separation, and sensor-based techniques for producing high-purity recycled glass (translated from Recyclingtechnik (Martens & Goldmann, 2016)).

A diagram of a typical container glass recycling facility is shown in Figure 9: Process flow for container glass cullet treatment, showing sorting, crushing, magnetic separation, and sensor-based techniques for producing high-purity recycled glass (Martens & Goldmann, 2016).

Although the textbook on Recyclingtechnik describes a typical procedure that involves the use of impact mills and suggests a particle size range of 5–60 mm for container glass cullet with the specific particle

distributions, it is important to emphasise that real practices can differ from those described in the textbook.

The glass crusher mentioned in the Green Combined Resource Recycling System for the Recycling of Waste Glass (Yao et al., 2021) is hammer crusher and aims feed particle size: 2−6 mm; 6−12 mm; 12−60 mm for the optical sorter. This can be determined as the adaptability of industrial recycling systems in terms of meeting the requirements in terms of either economic or operational requirements.

In conclusion, container glass recycling is a mature and highly efficient system that relies on:

- Accurate sorting,
- Advanced purification,
- Standardised input quality

to enable a closed-loop recycling process. Maintaining high cullet quality is key to maximising economic and ecological benefits.

2.4.5. Research and Development in Optical Sorting

While industrial container glass recycling is already highly standardised, research and development activities continue to focus on improving sorting efficiency and addressing technical limitations. In particular, optical sorting technologies have gained considerable attention in both academic and industrial contexts, as they enable high-throughput separation of cullet by colour and material type, thereby ensuring furnace-ready quality standards. Advanced sensor-based systems, including near-infrared (NIR) spectroscopy, X-ray fluorescence (XRF), and laser-induced breakdown spectroscopy (LIBS), are increasingly being investigated to complement or surpass conventional colour cameras (Lebullenger et al., 2019; Peukert et al., 2022).

Academic institutions play a central role in this development by providing controlled environments for experimental testing and prototype evaluation. Such platforms allow new approaches to be tested at a small scale before industrial application. These academic research activities are particularly important because they establish the link between theoretical process modelling and industrial practice. By simulating real-world sorting challenges in a contained environment, universities are able to develop and test solutions for persistent issues, such as detecting ceramics, porcelain, or heat-resistant glass fragments, as well as improving discrimination between closely related colour shades. The outcomes not only contribute to advancing scientific knowledge but also help bridge gaps between education and industry requirements in the field of sustainable resource management (*FEVE-Brochure-Recycling-Why-Glass-Always-Has-a-Happy-CO2-Ending*, n.d.; Lebullenger et al., 2019; Martens & Goldmann, 2016).

2.4.6. Particle Size Distribution (PSD) and Sauter Mean Diameter (SMD)

The particle size distribution (PSD) of cullets play a decisive role in glass recycling, as it affects melting behaviour, separation efficiency, and the quality of the final product. The particle size distribution (PSD) of the glass granulates was determined through dry sieving according to DIN standards. For a quantitative evaluation, both the cumulative distribution Q3(x) and the differential distribution q3(x) were calculated.

The cumulative distribution Q3(x) expresses the fraction of the total sample mass that passes through a sieve with mesh size x (Stieß, 2009):

$$Q_3(x) = \frac{Cumulative\ mass\ of\ particles\ smaller\ than\ x_i}{Total\ sample\ mass} \quad [1]$$

The differential distribution q3(x) corresponds to the proportion of the sample mass within a given size interval Δx, normalised by the interval width (Stieß, 2009):

$$q_3(\bar{x}_i) = \frac{\Delta Q_3(x_i)}{\Delta x_i} \quad [2]$$

where $\bar{x}_I$ represents the mean particle size of the interval.

From these distributions, the mean particle diameters can be derived using the general moment equation (Stieß, 2009):

$$D[a,b] = \frac{\sum n \cdot d^a}{\sum n \cdot d^b} \quad [3]$$

For the purpose of this study, the Sauter mean diameter (surface-area weighted mean diameter) was used, defined by a=3, b=2 (Stieß, 2009)

$$d_{32} = \frac{\sum n \cdot d^3}{\sum n \cdot d^2} \quad [4]$$

This parameter provides a meaningful representation of the particle system, as it relates the particle volume to its surface area.

2.4.7. Physical Properties Relevant to Recycling

In addition to particle size, the physical properties of cullet are of major importance for recycling processes. Parameters such as particle density, bulk density, tapped density, and porosity determine how the material behaves during handling, transport, and separation. These properties also affect the efficiency of fluid-based separation methods and the packing structure in bulk storage. A precise characterization of these values enables a better prediction of the material's flowability and suitability for subsequent recycling operations.

The particle density can be calculated with the following formula (Stieß, 1997):

$$\rho_{Particle} = \frac{mGlass}{VParticle} \quad [5]$$

The calculation of bulk density is based on the equation given below (Stieß, 1997):

$$\rho_{Bulk} = \frac{mGlass}{VGlass} \quad [6]$$

For the determination of tapped density, the following formula was applied (Stieß, 1997):

$$\rho_{Tapped} = \frac{me\ Glass\ (end)}{Ve\ Glass\ (end)} \quad [7]$$

Porosity was calculated theoretically based on the relationship between bulk density and particle density using the following formula (Stieß, 1997):

$$Porosity = 1 - \frac{Bulk\ density}{Particle\ density} \quad [8]$$

In addition to determine the porosity of granular media such as crushed glass, fluidized bed experiments can be conducted by observing the pressure loss behaviour as a function of superficial gas velocity. The setup consists of a vertical column filled with particulate material, through which air is passed from below at increasing flow rates.

The pressure drop across the bed exhibits three distinct regimes, as illustrated in Figure 10**.**

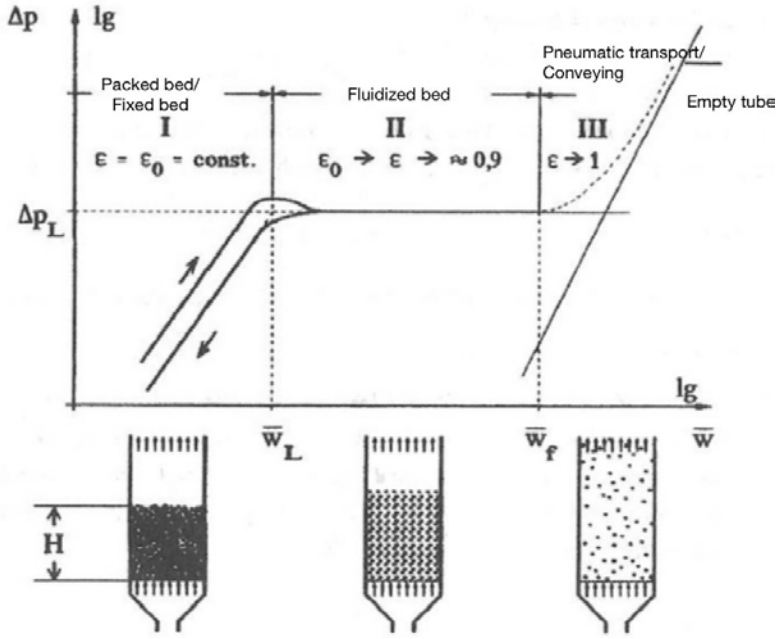

Figure 10: Pressure drop curve of a fluidized bed, illustrating fixed bed, fluidized bed, and pneumatic transport regimes (translated from Mechanische Verfahrenstechnik 2 (Stieß, 1997)).

Region I: Packed Bed (*Festbett*)

At low gas velocities, the bed remains stationary, and the gas percolates through the voids between particles. In this regime, the pressure drop increases linearly with superficial velocity and is strongly influenced by the packing structure and porosity. The porosity ε of the bed can be determined by fitting experimental data to the **Ergun equation** (Stieß, 1997):

$$\frac{\Delta\rho}{H} = 150 \cdot \frac{(1-\varepsilon_0)^2}{{\varepsilon_0}^3} \cdot \frac{\eta \cdot \varpi}{{d_{32}}^2} + 1{,}75 \cdot \frac{1-\varepsilon_0}{{\varepsilon_0}^3} \cdot \frac{\rho_f \cdot \varpi^2}{d_{32}} \qquad [9]$$

Region II: Fluidized Bed (*Fließbett*)

As airflow increases beyond the minimum fluidization velocity ϖ_L, the particles begin to lift and behave like a fluid. In this regime, the pressure drop stabilises and becomes nearly constant despite further increases in velocity. This transition marks the point at which fluidization begins and can be used to confirm whether the sample was fully fluidized (Stieß, 1997).

Region III: Pneumatic Transport

At very high velocities, particles are carried out of the bed, and pressure loss increases again. This regime is not used for porosity measurement (Stieß, 1997).

2.4.8. Measurement Uncertainty

Gaussian error propagation was used to handle measurement uncertainties. The general uncertainty for a function based on multiple variables is defined as (Bevington & Robinson, 2003; *DIN 1319-3:1996 – Grundlagen Der Messtechnik – Teil 3: Auswertung von Messungen Einer Einzelnen Messgröße Und von Mehreren Messgrößen Derselben Art*, 1996):

$$\Delta f = \sqrt{\left(\frac{\delta f}{\delta x_1}\Delta x_1\right)^2 + \left(\frac{\delta f}{\delta x_2}\Delta x_2\right)^2 + \cdots} \quad [10]$$

For density calculations depending on mass and volume, this reduces to:

$$\frac{\Delta \rho}{\rho} = \sqrt{\left(\frac{\Delta m}{m}\right)^2 + \left(\frac{\Delta V}{V}\right)^2} \quad [11]$$

All density measurements were based on the determination of sample mass and volume. Mass was determined using a Kern EW analytical balance with a measurement accuracy of ±0.01 g (KERN & SOHN GmbH, 2022). Unless otherwise stated, the volume was measured with a 500 mL graduated cylinder (scale division: 10 mL; measurement uncertainty: ±1 mL) (*DIN 1319-3:1996 – Grundlagen Der Messtechnik – Teil 3: Auswertung von Messungen Einer Einzelnen Messgröße Und von Mehreren Messgrößen Derselben Art*, 1996).

The measurement uncertainty of the pycnometer could not be specified due to the absence of manufacturer information. In line with (*DIN EN ISO 12154:2014 – Determination of Density by Gas Pycnometry (ISO 12154:2014)*, 2014), helium pycnometer generally achieves an accuracy of better than ±0.01 g/cm³, which was assumed in this study.

The tapped density was determined using a standardised tapping device (Engelsmann AG, Germany) with a 250 mL graduated cylinder (scale division: 1 mL; measurement uncertainty: ±1 mL).

3. Methods and Materials

In order to generate a standardised bulk material from recycled glass suitable for use in an optical sorting system and also optimised the recycling system, a structured and reproducible method was developed. The methodology applied was identical for both clear and green glass to ensure the comparability of results. The preparation procedure comprised several steps. First and foremost, the glass container needed to be cleaned of any residues and labels that were previously present. The cleaned glass container is then manually crushed with a hammer and subsequently processed via a sieve machine to ascertain the appropriate particle size. The excessively large glass cullet was then crushed using a mechanical crusher and re-sieved with a sieve machine. In the next steps, the samples were divided up, and the size of the particles was studied. The basic physical properties were also researched. The flow behaviour of the glass granulate is also studied to see if it can be handled and processed by machines in the future.

This chapter will go into more detail about all the methods used for this thesis. The materials employed in this experiment comprised post-consumer glass containers, namely clear (clear) glass and green glass, often known as "*Altglas*" in Germany. These specific types of glass were selected to illustrate the two principal colour categories relevant to optical sorting applications. Following the completion of any processing, the bottles were cleaned with simply the most fundamental of household materials, specifically dishwashing soap and hot water from the tap. For the purpose of simulating a low-resource

preparation process while also ensuring the removal of labels, adhesives, and surface residues from recycled glass, this straightforward cleaning approach that is also highly effective was selected.

Figure 11: Clear and green glass containers that were used for the research (author's own photograph).

3.1. Glass Cleaning

The glass containers were sanitised prior to any mechanical processing to remove external contaminants, including labels, adhesives, and residual contents. To achieve this objective, only the most basic cleaning agents for the household were employed, which are dishwashing soap and hot tap water. The contaminated glasses are first soaked in the hot water in to make the cleaning process easier.

Figure 12: Glass cleaning process (author's own photograph).

There wasn't much machinery used to clean the bottles by hand. This plan made sure that the process stayed possible and could be repeated and that the glass surfaces were thoroughly cleaned so that they could be handled and characterised later. Before moving on to the next step, the cleaned glass must be completely dry.

3.2. Glass Cullet Preparation: Glass Crushing

Prior to the cleaning of the glass bottles, they underwent mechanical processing, yielding cullet suitable for particle analysis and sorting. A range of manual and machine-assisted techniques were employed during the crushing process. Each method was evaluated for its efficacy in producing granulate within the required size range. The various crushing methods that were utilised in this investigation are broken down into more specific subsections below.

3.2.1. Hammer Crusher (Manual Crushing)

As a first step, the glass bottles were manually crushed using a standard metal hammer. This method allowed for the initial breakdown of the bulky bottle structure into manageable fragments. The procedure was carried out by taking the bottles and placing them in a container that provided protection, and then using a hand hammer to pound them repeatedly. Prior to the material being processed with mechanical equipment, this method, despite its simplicity, proved to be effective in pre-crushing the material and lowering its volume.

3.2.2. Jaw Crusher (*Backenbrecher*)

A jaw crusher, a mechanical apparatus commonly employed for the primary crushing of hard and brittle substances such as ores, minerals, and construction debris, was utilised to further process the already crushed glass cullets. Material is fragmented between a stationary jaw and a mobile jaw, resulting its reduction into smaller particles. This is the fundamental concept that governs its operation. The width of the space between the jaws can be adjusted, allowing for precise control over the resultant particle size (Stieß, 1997). The jaw crusher was employed after the manual pre-crushing process to produce a more homogeneous granulate suitable for sieving and further characterization. The machine was highly effective, as it managed brittle materials such as glass while generating minimal particle production. It proved to be an exemplary option for recycling processes conducted in a laboratory environment (Blanc, 1928). In this study, a **Retsch BB 200** (Figure 13) jaw crusher was used for the mechanical crushing (Retsch GmbH, 2025).

Figure 13: Retsch BB 200 jaw crusher source: (Retsch GmbH, 2025).

To examine the effect of discharge opening dimensions on particle output, three distinct jaw gap settings were evaluated: 2,5 mm; 5 mm; and 7 mm. The gap widths are the distances between the fixed and moving jaws at their closest point, and they have a direct effect on the size distribution of the resulting granulate. Changing the size of the jaw opening leads to changes of the crushing process so that the pieces are the right size for further sifting and examination. It was then chosen as the main crushing tool for this study since it worked well and was dependable.

The dependability of the jaw crusher is evidenced by its application across several sectors, including mining, metallurgy, recycling, and materials research.

3.2.3. Cutting Mill (*Schneidmühle*)

To evaluate alternative crushing performance, a **Retsch SM 2000** cutting mill (Figure 14) was also tested for processing the crushed glass cullets. The machine operates through a shearing mechanism, which means it uses high-speed revolving blades, and it features a double cutting bar system as shown in Figure 15 to improve cutting efficiency.

Figure 14: Cutting Mill SM2000, HAW Hamburg (author's own photograph).

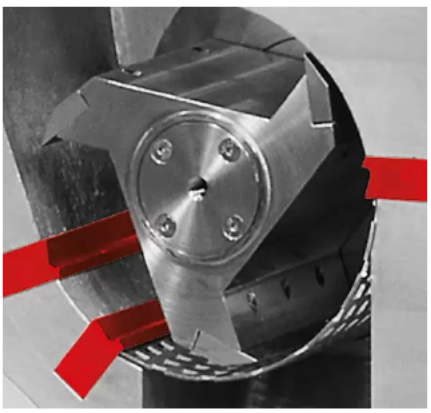

Figure 15: Double cutting bar system and bottom sieve of cutting mill (Retsch GmbH, 2025).

For this experiment, the cutting mill was operated with a bottom sieve of 20 mm perforations to define the desired maximum output size.

While the SM 2000 offered high-speed processing and clean, uniform cuts, its performance on brittle glass was less ideal. The machine tended to produce a higher proportion of fines and glass dust compared to the jaw crusher. In addition, the hard and angular structure of the glass shards led to clogging as well as an increase in wear.

3.3. Sample Division

After the glass was crushed, the resulting cullet was divided into equal portions using a **riffle splitter** (Figure 16). This device ensures that the subsamples are statistically representative of the original bulk material by guiding the particles alternately through a series of equally spaced chutes. The goal of using the riffle splitter in this study was to decrease sampling bias and ensure that all of the following analyses—sieving, density, porosity, and flowability—were done on the same, comparable material.

Figure 16: Riffle Splitter, HAW Hamburg (author's own photograph).

According to DIN 66165, the sample mass used for sieve analysis must be carefully controlled to avoid overloading of the sieve surface, as this can lead to inaccurate or non-reproducible results. A much lower mass, around 50 g, is generally what the standard calls for. This depends on the type of material and the size of the mesh. Glass has a high bulk density, so this study used a sample mass of about 300 g. The sieve tower also needs a certain amount of room for optimal layering. This procedure is an intentional departure from the DIN rule, which says that there must be enough samples to make sure that the results are accurate for the big and heavy glass granulates.

3.4. Particle Size Distribution Analysis

To determine the particle size distribution of the crushed glass material, multiple sieving procedures were carried out using different equipment and sieving principles. The aim was both to compare the crushing methods (jaw crusher vs. cutting mill) and to define the standardised particle range (4–10 mm) used in subsequent tests.

3.4.1. Sieving Method and Equipment

A series of dry sieving procedures was carried out using two different laboratory-scale sieve systems. Both systems employed a sieving tower (*Siebturm*) but varied in their mechanical motion and sieving dynamics. The first system was a **Retsch AS200 vibratory sieve shaker (**Figure 17**)** featuring a tossing motion (*Wurfsiebung*), which combines vertical and circular movements to accelerate particles and enhance the passage through mesh openings (Retsch GmbH, 2025). A fixed amplitude of 0,6 mm and 6 minutes of total sieving duration were used for the study with this device.

Figure 17: Sieving tower (Retsch GmbH, 2025).

The second device was a **analyser sieve shaker from Fritsch GmbH (**Figure 18**)**, that used a planar motion (*Plansiebung*), where particles are distributed across the sieve surface in a horizontal pattern. The total sieving duration was also set to 6 minutes. The vibration intensity on this device is adjustable and given on a scale from 1 to 10. A setting vibration of level 5 was selected to ensure effective separation of the glass particles without overloading or excessive fragmentation.

Figure 18: Sieving tower from Fritsch GmbH, HAW Hamburg (author's own photograph).

In the course of preliminary testing, both systems were employed to conduct an analysis of the identical glass material. Due to the effect of vertical acceleration, elongated glass culets—particularly those with narrow cross-sections and extended lengths—tended to flow more easily through the mesh layers of the Retsch device. Consequently, a greater number of larger particles were found in the finer fractions. The Fritsch planar motion system demonstrated a superior ability to retain elongated particles, resulting in a more precise separation that is based on actual particle width. The Fritsch sieving system was chosen for all final measurements due to this rationale.

3.4.2. Preliminary Comparison: Jaw Crusher vs. Cutting Mill

In order to assess the effect of the crushing method on particle size distribution, a preliminary sieving comparison was conducted using a standardised sieve tower (*Siebturm*). Glass cullet samples produced by the jaw crusher and the cutting mill were separately analyzed using a stack of sieves with **mesh sizes of 4,0 mm; 4,5 mm; 5,0 mm; 5,6 mm; 6,7 mm; and 10,0 mm**. A notably large sample mass was used during this comparison, exceeding typical DIN-recommended amounts, to achieve representative separation across all sieve layers despite the material's density. Each sample was dry-sieved under controlled conditions, and the retained mass on each mesh was recorded. The goal of this comparison was to evaluate which crushing method provided a particle size distribution that better aligned with the target range of 4–10 mm for the intended optical sorting application. Observations from this analysis informed the selection of the jaw crusher as the preferred crushing method due to its ability to produce a narrower and more controlled particle size distribution.

3.4.3. Final Sieving Procedure for Standardised Granulate

After dividing the glass cullets from the jaw crusher into representative samples using a riffle splitter, the final particle size distribution was determined with the Fritsch sieve system with a comprehensive selection of sieves with **mesh sizes of 4,0 mm; 4,5 mm; 5,0 mm; 5,6 mm; 6,7 mm; 10,0 mm; and 11,2 mm.** This range selection facilitated the elimination of both overly fine and large particles while offering a comprehensive understanding of the granulate's gradation. Particles retained on the 4 mm and 10 mm sieves were designated as the standardised fraction for subsequent physical property evaluation. The use of the 11,2 mm top sieve ensured that particles exceeding the upper limit were measured and excluded.

3.5. Physical Property Measurements

To characterise the physical behaviour of the standardised glass granulate, a series of measurements was carried out, including particle density, bulk density, tapped density, and porosity. Each parameter was determined using both conventional manual methods and precision instruments to allow for data comparison and validation.

3.5.1. Particle Density

Particle density was measured using two methods. In the manual approach, the water displacement method was utilised. This method involved placing a known quantity of granulate into a graduated

cylinder that was only partially filled with water when the process was carried out. The volume increase caused by the sample was recorded, and particle density was calculated as the ratio of mass to displaced volume.

To complement this, a gas pycnometer was used for higher precision. The instrument determines the actual particle volume by quantifying the pressure variation induced by helium gas displacement. This technique mitigates the impact of surface flaws or interior voids that may be neglected in the water displacement method, providing a more precise assessment of actual material density.

Figure 19: Gas pycnometer, HAW Hamburg (author's own photograph).

3.5.2. Bulk Density

The bulk density was assessed by lightly filling a measuring cylinder with the glass granulate without exerting any compression. The sample's mass was divided by the total volume it occupied within the cylinder. This measurement indicates the material's behaviour under free-pour conditions and is pertinent for transportation, storage, and dosage applications.

3.5.3. Tapped Density

The tapped density was determined by inserting the sample into a graded cylinder and applying repetitive mechanical tapping using a standardised equipment. The procedure persisted until no additional decrease in volume was noted.

The final volume was documented, and the tapped density was determined by dividing the mass of the sample by the settled volume. This metric denotes the compatibility and flow potential of the material under dynamic conditions.

Figure 20 shows the device that was used for the tapped density measurement.

Figure 20: Device used for tapped density measurement, HAW Hamburg (author's own photograph).

3.5.4. Porosity

Porosity was calculated theoretically based on the relationship between bulk density and particle density using the formula [8].

To determine the porosity of the crushed glass particles, an additional method involving a fluidized bed equipment was utilised (Figure 21).

Figure 21: fluidized bed equipment, HAW Hamburg (author's own photograph).

The setup involved the upward flow of air through a cylindrical column filled with the granular material. By varying the volumetric airflow rate and measuring the corresponding pressure drop across the fixed

bed, it was possible to derive porosity through mathematical modelling. The pressure drop data was obtained using a U-tube manometer and a digital sensor, while the superficial gas velocity was calculated based on the known volumetric flow rate and the cross-sectional area of the bed. The experimental conditions correspond to the fixed bed regime (*Festbett Bereich*), where the granular bed remains stationary, and the interstitial flow governs the pressure loss.

Only measurements taken within the fixed bed range were considered valid for the glass porosity determination. The Ergun equation was applied, which relates the pressure drop to the bed porosity, particle diameter, gas viscosity and density, and superficial velocity (formula [9]).

Since the equation is non-linear with respect to porosity, it cannot be solved analytically. Therefore, numerical iteration was employed (using Excel's goal-seek function) to match the calculated pressure drop to the experimental values and derive the corresponding porosity values.

3.5.5. Flowability

The flowability of the glass granulate was determined for its handling characteristics during storage, transportation, and mechanical feeding processes. Flowability is an important characteristic of bulk materials, especially when the material is designed for automated systems like optical sorting lines or dosing units.

This study evaluated flow behaviour with a Fritsch Labor vibrating chute (Figure 22), featuring an adjustable funnel at the feeding portion. The granulate was introduced via a broad plastic funnel that channelled the material into the vibrating metal chute. The material's capacity to move through the sloping surface smoothly and discharge into a collection container was observed. Particular focus was set on the geometry and dimensions of the funnel opening. A wide funnel was chosen to mitigate the risk of clogging or arching, a frequent issue associated with unevenly shaped glass particles.

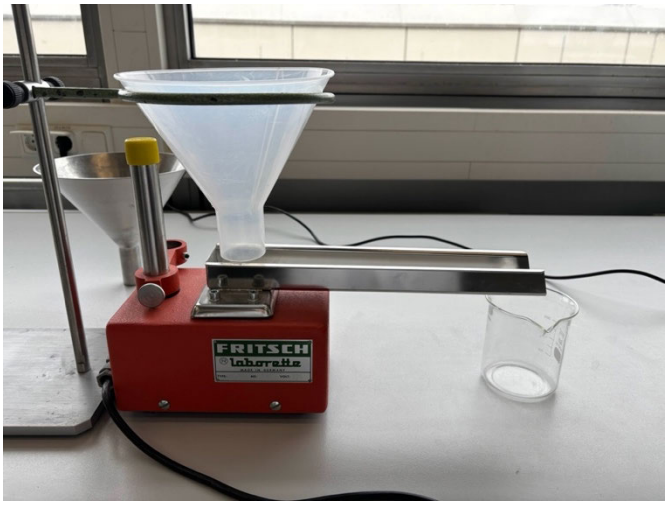

Figure 22: Vibrating chute from Fritsch Labor, HAW Hamburg (author's own photograph).

Figure 23 shows the glass particles during testing in the vibrating chute prototype.

Figure 23: Glass particles in the vibrating chute prototype (author's own photograph).

3.6. Sample Mixture Preparation

After crushing and sieving, the final step in sample preparation was the controlled mixing of clear and green cullet. To obtain representative material for subsequent optical sorting research, a mixture was created consisting of approximately 95% clear glass and 5% green glass. This ratio reflects typical conditions in container glass recycling, where flint glass dominates the input stream, but small proportions of coloured glass are present.

The mixture was prepared by weighing the respective cullet fractions after sieving (4–10 mm). The measured volumes were homogenised by repeated manual mixing in a large container to ensure uniform distribution of the two glass types.

4. Results

This chapter presents the experimental results obtained from the processing and characterization of the glass samples. The results are organised in accordance with the sequence of the procedures that were applied, beginning with the comparison of crushing techniques and continuing on to the measurement of particle size distribution and physical parameters such as the density of the particles and the bulk, porosity, and flowability and ending with the flowability of the material. Note: In the tables and figures, commas are used as decimal separators in accordance with German numerical formatting.

4.1. Particle Size Distribution

The particle size distribution (PSD) study took place to determine the size classes of the crushed glass and to assess the effectiveness of the various comminution techniques that were applied. In the following, the PSD is displayed as both a cumulative (*Verteilungssumme*) and a differential (*Verteilungsdichte*) distribution curve. The cumulative distribution gives the information about

distinctive particle size thresholds, for example, d50. In the other hand, the differential distribution emphasises the dominant particle size fractions.

4.1.1. Comparison of Crushing Techniques

The following section compares the particle size distributions obtained from various crushing techniques.

4.1.1.1. Hammer Crushing (Manual)

In addition to the mechanical comminution methods, the glass was also manually crushed using a hammer. As shown in Figure 24: clear (left) and green (right) glass samples after manual hammer crushing (author's own photograph). This method produced a broad distribution with a considerable share of oversized fragments.

Figure 24: clear (left) and green (right) glass samples after manual hammer crushing (author's own photograph).

The cumulative and differential particle size distributions are presented for both clear and green glass. Figure 25 shows the cumulative PSD for hammer-crushed clear and green glass, while Figure 26 presents the corresponding differential distributions.

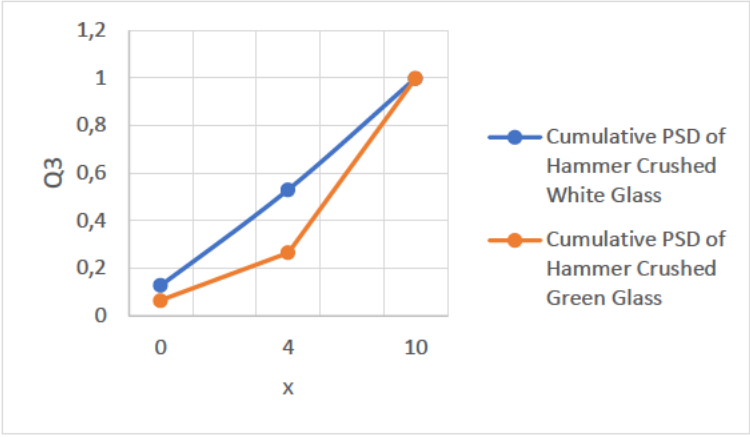

Figure 25: Cumulative PSD of hammer-crushed clear and green glass.

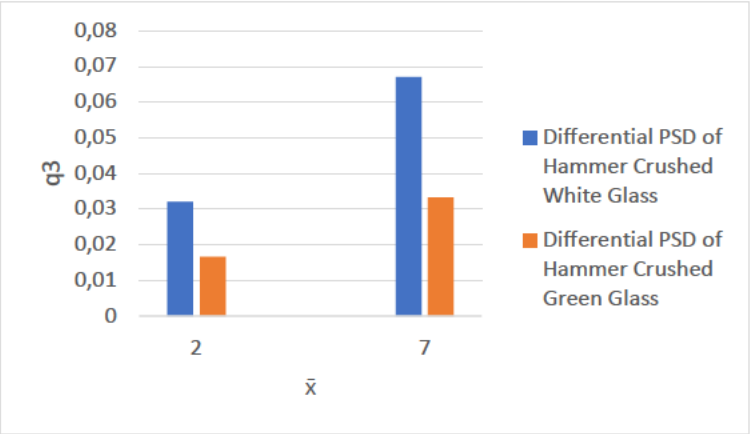

Figure 26: Differential PSD of hammer-crushed clear and green glass.

4.1.1.2. Jaw Crusher

The particle size distribution of glass crushed with the jaw crusher at different gap settings (2,5 mm; 5 mm; and 7 mm) is illustrated below. Both cumulative and differential curves are provided to emphasize the influence of the jaw gap on the resulting particle size fractions.

Figure 27 shows the cumulative PSDs of jaw-crushed glass at gap settings of 2,5 mm; 5 mm; and 7 mm, while Figure 28 presents the corresponding differential distributions.

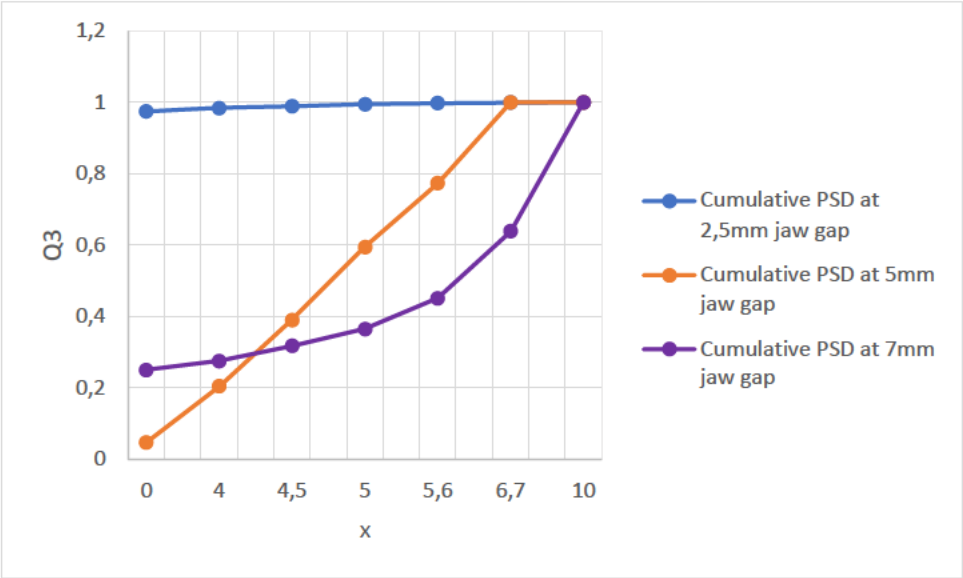

Figure 27: Cumulative PSD of jaw-crushed glass at 2,5mm; 5mm; 7mm jaw gaps.

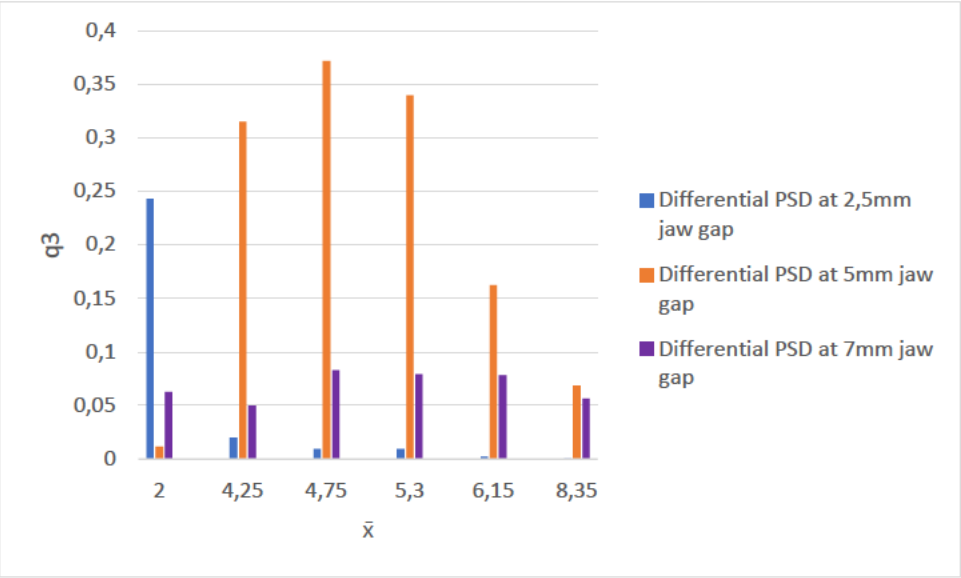

Figure 28: Differential PSD of jaw-crushed glass at 2,5; 5mm; 7mm jaw gaps.

Figure 29, Figure 30, and Figure 31 depict representative samples of jaw-crushed glass for the different gap settings. For comparison, only the clear glass samples are presented, since they adequately illustrate the influence of the jaw gap and serve as the reference material for the subsequent evaluation of the crushing techniques.

Figure 29: Jaw-crushed glass sample at 2,5 mm jaw gap (author's own photograph).

Figure 30: Jaw-crushed glass sample at 5 mm jaw gap (author's own photograph).

Figure 31: Jaw-crushed glass sample at 7 mm jaw gap (author's own photograph).

4.1.1.3. Cutting Mill

Figure 32 and Figure 33 show the cumulative and differential particle size distributions of glass crushed with the cutting mill using a 20 mm sieve. Two separate batches were analysed to verify the reproducibility of the results.

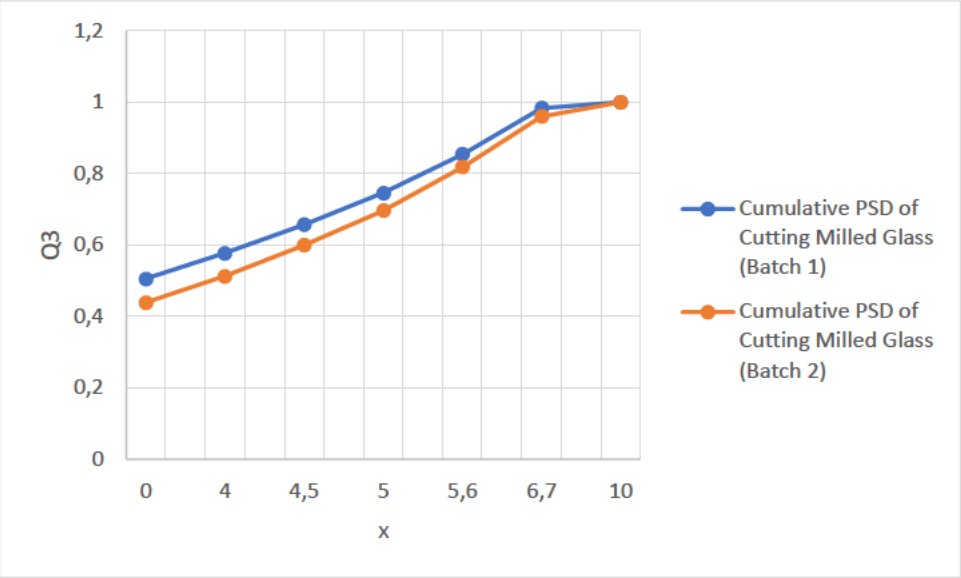

Figure 32: Cumulative PSD of cutting-milled glass with 20 mm sieve (Batch 1 and 2).

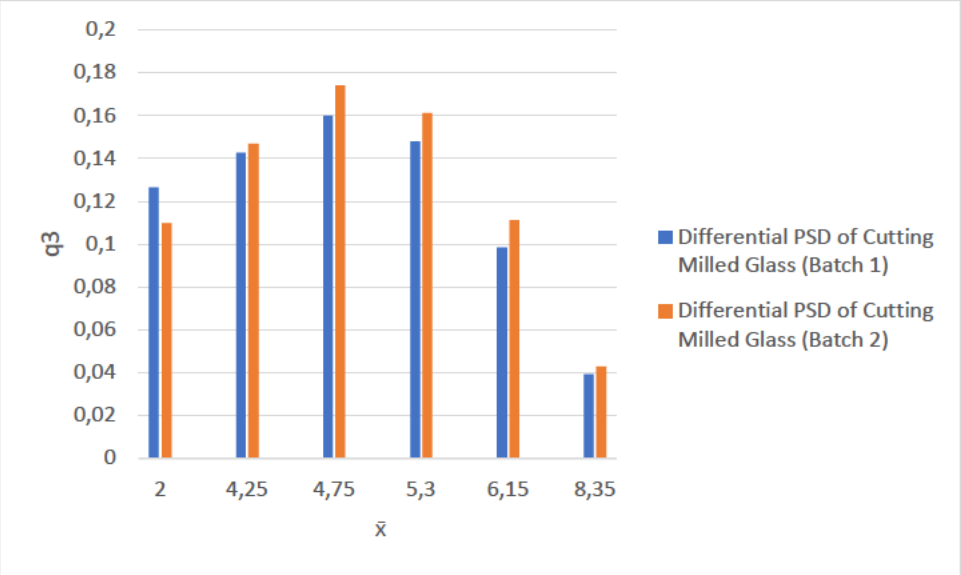

Figure 33: Differential PSD of cutting-milled glass with 20 mm sieve (Batch 1 and 2).

Figure 34 depicts representative samples of the two cutting mill batches. The images are provided to illustrate the visual similarity of the fragmentation outcome.

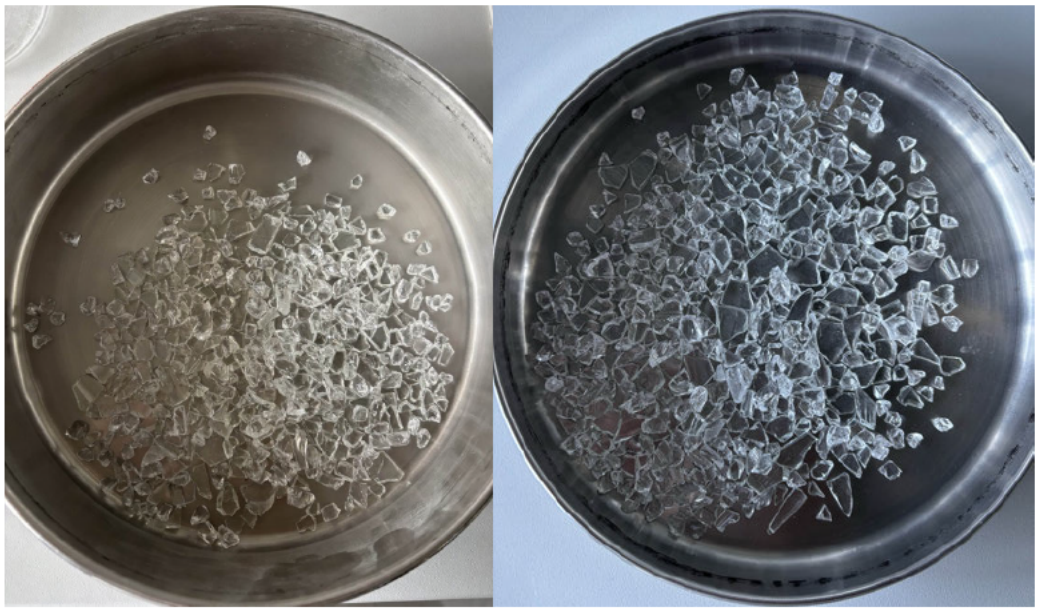

Figure 34: Cutting-milled glass sample with 20mm sieve, batch 1 (left) and batch 2 (right) (author's own photograph).

4.1.2. Clear and Green Glass

In the following, the particle size distributions of clear and green glass are presented. Both materials were processed with the jaw crusher at a gap setting of 7 mm. Figure 35 shows the cumulative PSDs of clear and green glass, while Figure 36 presents the corresponding differential distributions. These diagrams provide the quantitative basis for comparing the two glass types.

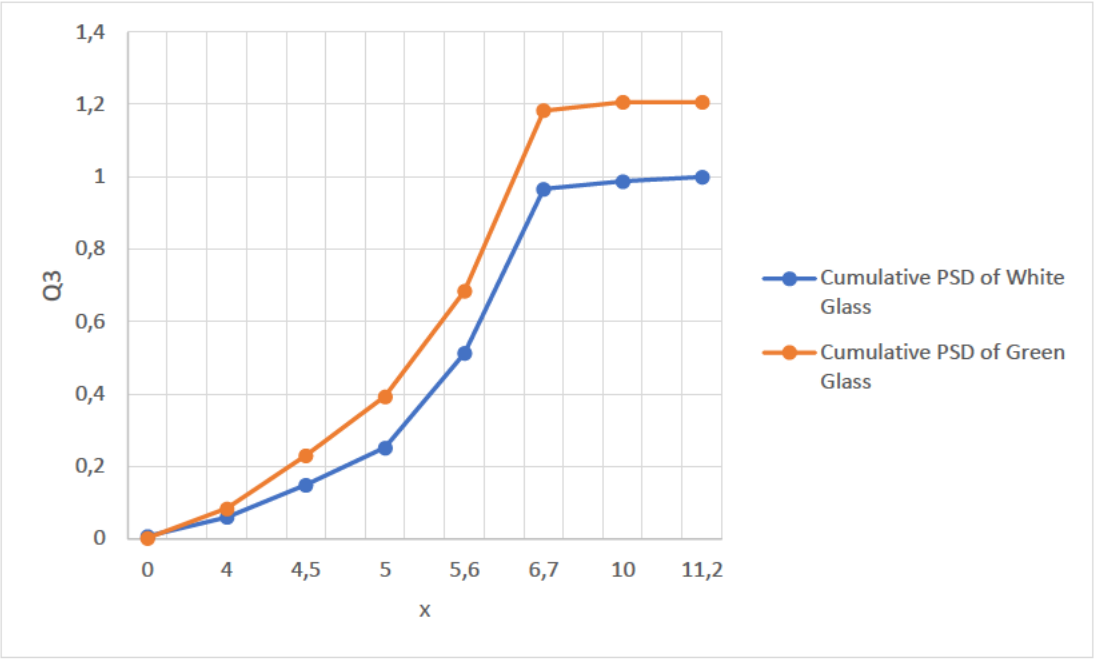

Figure 35: Cumulative PSD of clear and green glass.

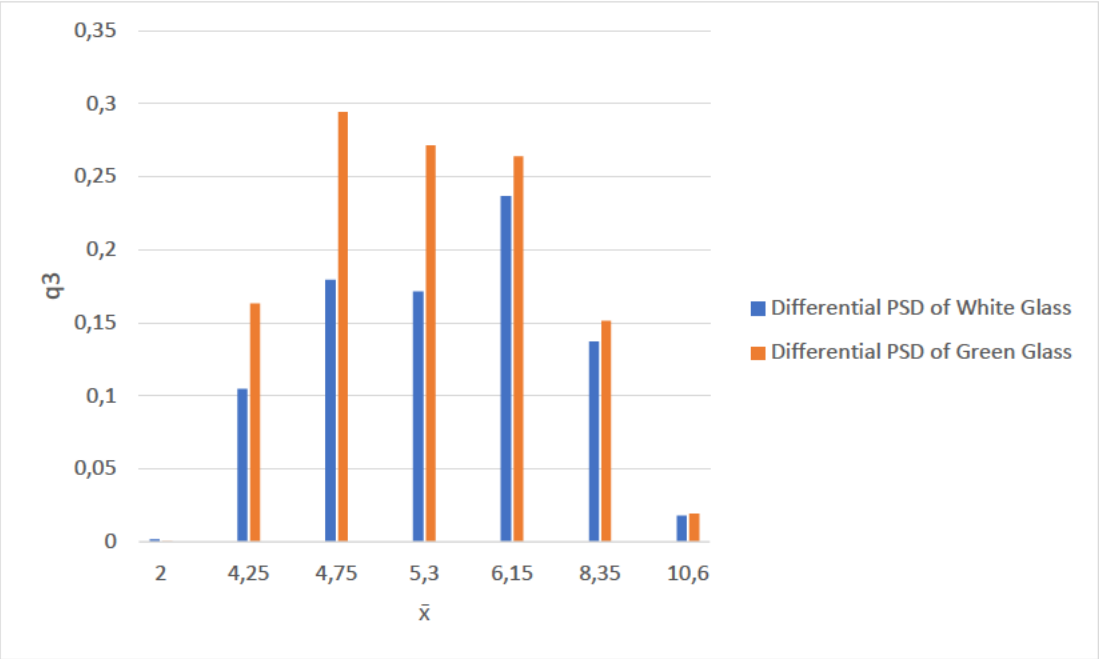

Figure 36: Differential PSD of clear and green glass.

Figure 37 and Figure 38 display the sieved fractions of clear and green glass according to DIN. Before sieving, the samples were divided using a riffle splitter to ensure representative subsampling. The images provide a visual comparison of the particle size classes obtained from both materials.

Figure 37: clear glass sample according to DIN (author's own photograph).

Figure 38: Green glass sample according to DIN (author's own photograph).

The detailed calculation steps for the presented results are provided in the Appendix.

4.2. Physical Properties

In addition to the distribution of particle sizes, the characterization of the crushed glass also includes the determination of its physical qualities. The structure and packing behaviour of a material can be better comprehended by studying parameters such as particle density, tapped density, and bulk density. These qualities do not only represent the fundamental characteristics of the glass particles but also impact how they are handled, how easily they flow, and how suitable they are for recycling operations that will occur in the future.

4.2.1. Particle Density

The particle density of the glass samples was determined using two approaches: the manual water displacement method and the helium gas pycnometer. The manual method provided an accessible estimation of the density values, while the pycnometer offered higher precision.

4.2.1.1. Manual Method

Using the manual water displacement method, the particle density of clear and green glass is presented in Table 6.

$\rho_{Water} = 1000\ kg/m^3$

$V_1\ (V_{Glass}) = 500\ cm^3$

$V_2\ (V_{Water}) = \frac{(m2-m1)}{\rho water}$

$V_{Particle} = V_1 (V_{Glass}) - V_2 (V_{Water})$

Table 6: Particle density of clear and green glasses with the manual method.

Glass Type	m_1 (m_{Glass}) in grams	m_2 ($m_{water+glas}$) in grams	V_2(V_{water}) in cm^3	$V_{Particle}$ in cm^3	$\rho_{Particle}$ in g/cm^3
Clear	719,1	951,38	232,28	267,72	2,686
Green	706,67	945,34	238,67	261,33	2,704

With

Δm= 0,01 g

ΔV= 1 cm^3

The reliability of the determined densities was assessed by accounting for the measurement uncertainties of mass and volume, which were propagated using Gaussian error calculation (formula [11]).

$$\Delta\rho_{white} = \sqrt{\left(\frac{0{,}01g}{719{,}1g}\right)^2 + \left(\frac{1cm^3}{267{,}72cm^3}\right)^2} \cdot 2{,}686\frac{g}{cm^3} = 0{,}01\frac{g}{cm^3}$$

$$\Delta\rho_{green} = \sqrt{\left(\frac{0{,}01g}{706{,}67g}\right)^2 + \left(\frac{1cm^3}{261{,}33cm^3}\right)^2} \cdot 2{,}704\frac{g}{cm^3} = 0{,}01\frac{g}{cm^3}$$

Final uncertainty of particle density:

$$\rho_{white} = 2{,}69 \pm 0{,}01\frac{g}{cm^3}$$

$$\rho_{green} = 2{,}70 \pm 0{,}01\frac{g}{cm^3}$$

4.2.1.2. Gas Pycnometer

In addition to the manual approach, helium gas pycnometer was applied to determine the particle density with higher precision. The results are summarised in Table 7.

Table 7: Particle density of clear and green glasses with gas pycnometer.

Glass Type	$m_{Pycnometer\ (empty)}$ in grams	$m_{Total\ (Pycnometer+Glass)}$ in grams	$\rho_{Particle}$ in g/cm^3
Clear	6,90	19,56	2,293
Green	6,90	18,94	2,309

The reliability of the pycnometer results was assessed by accounting for the measurement uncertainty provided in literature and manufacturer specifications. Helium gas pycnometry generally achieves an accuracy of about ±0.01 g/cm³ (ISO 12154:2014). Accordingly, the uncertainty of the measured densities was taken as ±0.01 g/cm³.

Final uncertainty of particle density (Gas pycnometer):

$$\rho_{white} = 2{,}29 \pm 0{,}01 \frac{g}{cm^3}$$

$$\rho_{green} = 2{,}31 \pm 0{,}01 \frac{g}{cm^3}$$

4.2.2. Bulk Density

The bulk density of the clear and green glass samples was also determined by filling a 500 mL graduated cylinder without compaction. The ratio of sample mass to occupied volume provided the density values shown in Table 8.

Table 8: Bulk density of clear and green glasses.

Glass Type	m_{Glass} in gramm	V_{Glass} in cm^3	ρ_{Bulk} in g/cm^3
Clear	663,77	500	1,327
Green	682,90	500	1,366

With

Δm= 0,01 g

ΔV= 1 cm^3

The reliability of the determined densities was also assessed by accounting for the measurement uncertainties of mass and volume, which were propagated using Gaussian error calculation (formula [11]).

$$\Delta\rho_{white} = \sqrt{\left(\frac{0{,}01g}{663{,}77g}\right)^2 + \left(\frac{1cm^3}{500cm^3}\right)^2} \cdot 1{,}327 \frac{g}{cm^3} = 0{,}003 \frac{g}{cm^3}$$

$$\Delta\rho_{green} = \sqrt{\left(\frac{0{,}01g}{682{,}90g}\right)^2 + \left(\frac{1cm^3}{500cm^3}\right)^2} \cdot 1{,}366 \frac{g}{cm^3} = 0{,}003 \frac{g}{cm^3}$$

Final uncertainty of bulk density

$$\rho_{white} = 1{,}327 \pm 0{,}003 \frac{g}{cm^3}$$

$$\rho_{green} = 1{,}366 \pm 0{,}003 \frac{g}{cm^3}$$

4.2.3. Tapped Density

To evaluate the tapped density, the samples were placed in a 250 cm^3 graduated cylinder and subjected to repetitive mechanical tapping until the volume stabilised. The results for both clear and green glass are presented in Table 9.

Table 9: Tapped density of clear and green glasses.

Glass Type	$m_{0\ Glass\ (Start)}$ in grams	$V_{0\ Glass\ (Start)}$ in cm^3	$m_{e\ Glass\ (End)}$ in grams	$V_{e\ Glass\ End}$ in cm^3	ρ_{Tapped} in g/cm^3
Clear	333,93	250	333,93	248	1,346
Green	349,56	250	349,56	246	1,421

To evaluate the reliability of these results, the uncertainties of both mass and volume were considered. Mass was measured with the Kern EW analytical balance ($\Delta m = 0{,}01$ g), and the volume with a 250 cm^3 graduated cylinder ($\Delta V = 1\ cm^3$). Using Gaussian error propagation:

$$\Delta\rho_{white} = \sqrt{\left(\frac{0{,}01g}{333{,}93g}\right)^2 + \left(\frac{1cm^3}{248cm^3}\right)^2} \cdot 1{,}346\frac{g}{cm^3} = 0{,}005\frac{g}{cm^3}$$

$$\Delta\rho_{green} = \sqrt{\left(\frac{0{,}01g}{349{,}56g}\right)^2 + \left(\frac{1cm^3}{248cm^3}\right)^2} \cdot 1{,}421\frac{g}{cm^3} = 0{,}006\frac{g}{cm^3}$$

Final uncertainty of particle density:

$$\rho_{white} = 1{,}346 \pm 0{,}005\frac{g}{cm^3}$$

$$\rho_{green} = 1{,}421 \pm 0{,}006\frac{g}{cm^3}$$

4.2.4. Porosity

In addition to density, porosity was evaluated because it directly influences packing efficiency, flowability, and the behaviour of glass particles in recycling processes.

4.2.4.1. Manual Method

Porosity was calculated from the ratio of bulk to particle density, providing an indication of the void fraction within the packed glass granulates. The calculated values for porosity of clear and green glass are summarised in Table 10.

Table 10: Porosity of clear and green glasses with the manual method.

Glass Type	ρ_{Bulk} in g/cm^3	$\rho_{Particle}$ in g/cm^3	ε
Clear	1,327	2,293	0,421
Green	1,366	2,309	0,408

To quantify the reliability of the porosity values, the uncertainties of both bulk and particle density were propagated using Gaussian error calculation. The general expression is given by:

$$\Delta\varepsilon = \sqrt{\left(\frac{\delta\varepsilon}{\delta\rho_{bulk}} \cdot \Delta\rho_{bulk}\right)^2 + \left(\frac{\delta\varepsilon}{\delta\rho_{particle}} \cdot \Delta\rho_{particle}\right)^2}$$

With:

$$\frac{\delta\varepsilon}{\delta\rho_{bulk}} = -\frac{1}{\rho_{particle}} \; and \; \frac{\delta\varepsilon}{\delta\rho_{particle}} = -\frac{\rho_{bulk}}{\rho^2{}_{particle}}$$

Clear Glass

$$\frac{\delta\varepsilon}{\delta\rho_{bulk}} = -\frac{1}{2{,}293} = -0{,}436$$

$$\frac{\delta\varepsilon}{\delta\rho_{particle}} = \frac{1{,}327}{(2{,}293)^2} = 0{,}253$$

$$\Delta\varepsilon = \sqrt{(-0{,}436 \cdot 0{,}003)^2 + (0{,}253 \cdot 0{,}01)^2} = 0{,}003$$

Green Glass

$$\frac{\delta\varepsilon}{\delta\rho_{bulk}} = -\frac{1}{2{,}309} = -0{,}433$$

$$\frac{\delta\varepsilon}{\delta\rho_{particle}} = \frac{1{,}366}{(2{,}209)^2} = 0{,}256$$

$$\Delta\varepsilon = \sqrt{(-0{,}433 \cdot 0{,}003)^2 + (0{,}256 \cdot 0{,}01)^2} = 0{,}003$$

Final uncertainty of particle density:

$$\varepsilon_{white} = 0{,}421 \pm 0{,}003$$
$$\varepsilon_{green} = 0{,}408 \pm 0{,}003$$

4.2.4.2. Fluidized Bed

Based on the measured values and through the application of the Ergun equation (as described in Chapter 3), porosity values were estimated using an iterative numerical approach.

The bed height H during all clear glass measurements was measured and fixed at H_{clear}= 6,8 cm and H_{green}= 6,7 cm. Air at room temperature was used as the fluidizing medium. The dynamic viscosity and density of air were $\eta = 1{,}8 \cdot 10^{-5}$ Pa·s and ρ_f= 1,2 kg/m³ (Verein Deutscher Ingenieure, 2013). The Sauter

mean diameter d_{32} of the glass particles was estimated from particle size distribution to be approximately $d_{32clear}$= 0,0077 m and $d_{32green}$= 0,0074 m.

Measured pressure drop data were collected at different superficial gas velocities. For each data point, an iterative calculation was performed to determine the value of ε_0 that would best fit the measured pressure drop using the Ergun equation. Data points with zero pressure drop were excluded from this analysis.

A summary of the main results is presented below in Table 11.

Table 11: Summary of calculated porosity of clear glass and related parameters from fluidized bed experiments.

Float Body in mm	Volumetric Flow in l/min	Δh in mm	Δp in Pa	$\bar{w}$ in m/s	Δp Fixed Bed in pa	Porosity ε
6	2,174	17,000	166,770	0,002	0,000	
14	3,636	29,000	284,490	0,004	9,810	0,100
27	4,305	49,000	480,690	0,005	39,240	0,069
63	6,991	104,000	1020,240	0,008	0,000	
89	13,885	153,000	1500,930	0,015	9,810	0,155
120	19,587	220,000	2158,200	0,021	0,000	
150	30,273	292,000	2864,520	0,033	0,000	
200	40,884	446,000	4375,260	0,044	58,860	0,132

Table 12: Summary of calculated porosity of green glass and related parameters from fluidized bed experiments.

Float Body in mm	Volumetric Flow in l/min	Δh in mm	Δp in Pa	$\bar{w}$ in m/s	Δp Fixed Bed in pa	Porosity ε
6	2,204	17,000	166,770	0,002	0,000	
14	3,685	29,000	284,490	0,004	9,810	0,100
27	4,525	49,000	480,690	0,005	39,240	0,069
63	6,922	104,000	1020,240	0,007	0,000	
89	14,183	153,000	1500,930	0,015	9,810	0,155
120	19,610	220,000	2158,200	0,021	0,000	
150	30,513	292,000	2864,520	0,033	0,000	
200	50,048	446,000	4375,260	0,054	58,860	0,132

The pressure drop Δp across the fixed bed was determined by subtracting the baseline pressure drop measured in the empty fluidization column (Δp_{empty}) from the total pressure drop during the experiment. This correction is necessary, as the empty column setup also induces flow resistance due to the distributor plate and equipment geometry.

The values for the empty column measurements were recorded prior to filling the column and are listed in the appendix.

Additionally, the Sauter mean diameter (d_{32}) used in the Ergun equation was calculated from the data on particle size distribution data. The calculation procedure for d_{32}, as well as the baseline pressure drop values, can be found in the appendix.

4.2.5. Flowability

Several test variations verified that the chosen funnel configuration allowed continuous and freely flow. The analysis was principally qualitative, focusing on the observation of flow consistency and irregularities, including bridging or rapid motion. No direct measurement of flow rate was obtained; however, the configuration successfully mimicked actual handling situations. The test demonstrated the granulate's compatibility with gravity-fed systems, proving its suitability for later processing in automated settings.

4.3. Mixture Composition

To produce a representative cullet mixture for subsequent experiments, the sieved fractions of clear and green glass were combined in a controlled ratio. A total of 5,0 L of clear glass was mixed with 0,263 L of green glass, which corresponds to a ratio of approximately 95% clear glass and 5% green glass by volume. This ratio was chosen because it reflects typical conditions in glass recycling, where flint (clear) glass dominates but a small proportion of coloured glass is always present. The prepared cullet mixture of clear and green glass in the target 95/5 ratio is shown in Figure 39.

Figure 39: Final mixture of clear (95%) and green (5%) cullet fractions (author's own photograph).

5. Discussion

The following discussion interprets the obtained data, compares them with reference values from literature, and highlights their relevance for industrial recycling processes.

5.1. Particle Size Distribution

The PSD analysis highlights clear differences between the applied comminution methods. Manual hammer crushing resulted in a very broad size distribution with a significant share of oversized fragments. This reflects the uncontrolled energy input and random fracture patterns typical of manual impacts, making this method unsuitable for producing consistent cullets for recycling.

The jaw crusher showed a strong dependence on the gap setting. At 2,5 mm, the machine generated a large fraction of fines below 4–5 mm, resulting in dust-like particles that are often problematic in recycling plants. Increasing the gap to 5mm and 7mm progressively shifted the distributions toward coarser fractions, reducing the share of fines and producing more uniform particle classes. These trends align with the working principle of jaw crushers, where a narrower gap concentrates compressive stress and promotes extensive breakage, while a wider gap allows coarser fragments to pass through. From a recycling perspective, intermediate gap settings (5–7 mm) appear more favourable, since they provide a balance between efficient size reduction and the avoidance of excessive fines.

The cutting mill, by contrast, produced a relatively broad distribution with dominant coarse fractions. This is attributed to its shearing mechanism, where rotating blades fracture the brittle glass in an irregular way, producing elongated or splinter-like fragments and less control over the final size classes. Importantly, the cutting mill also generated a significant amount of fine dust due to secondary splintering of the glass, which accentuated the issue of fines already observed in the jaw crusher at narrow gaps. As a result, its output was both heterogeneous in size and problematic in terms of excessive fines. From the total of approximately 6 kg of glass processed, nearly half of the material ended up as fine dust (< 2 mm), indicating a considerable mass loss during milling.

Another important aspect observed in this study concerns the generation of fine fractions. Both the jaw crusher at narrower gaps (2,5 mm and 5 mm) and the cutting mill produced a considerable share of particles below 2–4 mm. Such fines are undesirable in the recycling context: they are prone to losses during handling, difficult to detect in optical sorting, and often discarded, which effectively reduces the usable cullet yield. For this reason, the jaw crusher with a 7 mm gap was preferred as the final crushing step in this work. This setting significantly reduced the amount of fines, while the resulting cullet remained within a representative size range for further sorting. This decision reflects a practical trade-off: avoiding excessive dust and material loss while still ensuring sufficient comminution for downstream processes.

When comparing glass types, both clear and green glass followed similar PSD trends under identical crushing conditions. However, green glass tended to retain slightly coarser fractions. This is consistent with compositional differences: green glass often contains higher iron oxide content, which increases hardness and mechanical resistance compared to flint glass. Similar observations are reported in the *Springer Handbook of Glass* (Lebullenger et al., 2019), where the mechanical strength of green glass is noted to be higher than that of clear glass, influencing its breakage behaviour.

From the viewpoint of industrial recycling, fines (<2 mm) are undesirable. They are poorly detected by optical sorting systems, easily lost during processing, and contribute to dust formation. Accordingly, most container glass plants aim to produce cullet in the range of 5–60 mm. This directly explains the widespread use of impact mills (*Prallmühlen*) in the industry, which represent the state-of-the-art technology for glass comminution (Martens & Goldmann, 2016). Unlike jaw or cutting mills, impact mills rely on high-speed rotors that project glass fragments against impact plates, producing angular particles with a relatively narrow distribution centred in the optimal range for sorting (Thomé-Kozmiensky & Hoffmann, 2010). Their output aligns precisely with the operational requirements of commercial sorting systems, such as Sesotec K9 or Binder+Co CLARITY, which are optimised for cullet fractions between ~5 and 60 mm.

Nevertheless, impact mills are not free from limitations. The high-energy fragmentation process inherently generates fine fractions below 4 mm, which require additional sieving and often lower material yield. The wear of blow bars and energy demand are further disadvantages compared to jaw crushers. Still, their ability to handle large volumes, produce furnace-ready cullet, and deliver consistent particle geometry explains their dominance in industrial container glass recycling.

In conclusion, the laboratory crushers applied in this study (jaw crusher and cutting mill) reproduced certain aspects of glass comminution but did not fully match industrial practice. While the jaw crusher at a 5–7 mm gap produced fractions closest to industrial requirements, the impact mill remains the reference technology for container glass recycling. The comparison underlines the importance of particle size distribution not only as a mechanical outcome but also as a decisive parameter for the efficiency of downstream sorting and remelting processes.

5.2. Particle Density

The particle density of the investigated glass samples was determined using both the manual water displacement method and helium gas pycnometer. The results ranged between 2,29 and 2,70 g/cm³, which is broadly consistent with literature values for soda-lime silicate glasses ranged between 2,4–2,6 g/cm³ (Doremus, 1994; Schaeffer, 2020; Shelby, 2005). The following discussion considers clear and green glass separately.

Clear Glass

For clear glass, the manual displacement method yielded 2,69 ± 0,01 g/cm³, whereas the pycnometer gave 2,29 ± 0,01 g/cm³. The manual method therefore produced a clear overestimation compared to the reference range. This can be explained by systematic issues of water displacement, including trapped air bubbles, incomplete wetting of angular particles, and reading uncertainties ISO 1183-1:2025 (International Organization for Standardization, 2025). The pycnometer result, while slightly lower than the expected values, is considered more reliable due to helium penetration into fine pores and the elimination of surface-tension effects (ISO 12154:2014) (International Organization for Standardization, 2014). Reported values for soda-lime flint glass are typically 2,45–2,55 g/cm (Doremus, 1994; Lebullenger et al., 2019; Shelby, 2005). Thus, the pycnometer value still confirms the classification as soda-lime glass, though it is shifted towards the lower end of the range.

Green Glass

For green glass, the manual method resulted in 2,70 ± 0,01 g/cm³, while the pycnometer gave 2,31 ± 0,01 g/cm³. The same systematic deviation was observed as for clear glass, with displacement producing

an overestimation and the pycnometer providing lower but more consistent values. Literature typically reports 2,48–2,56 g/cm³ for soda-lime green glass (Lebullenger et al., 2019; Schaeffer, 2020). The slightly higher density compared to flint glass is linked to the incorporation of Fe_2O_3 and other minor oxides used as colourants, which marginally increase the overall network density. The difference measured between clear and green glass in this study (≈0,02 g/cm³ by pycnometer) lies within the experimental uncertainty and is therefore not significant.

Implications for Recycling

From a recycling perspective, the measured densities confirm the classification of both clear and green cullet as soda-lime glass. Since the density contrast between different colours is minimal (<0.05 g/cm³), density-based methods are unsuitable for colour separation. This feature explains why optical sorting technologies are the industrial standard for container glass recycling (Martens & Goldmann, 2016). Nevertheless, particle density remains a relevant parameter for evaluating melt behaviour, batch design, and quality control in cullet processing.

5.3. Bulk Density

The bulk density values of the investigated samples ranged between 1,33 and 1,37 g/cm³, which are significantly lower than the particle densities (≈2,3–2,7 g/cm³). This discrepancy reflects the presence of interparticle voids when the material is loosely poured into a container without compaction. Bulk density therefore provides insight not only into the material's inherent density but also into its packing efficiency and flowability.

Clear Glass

For clear glass, a bulk density of 1,327 ± 0,003 g/cm³ was determined. This value is well within the typical range reported for soda-lime flint cullet, which lies between 1,2 and 1,4 g/cm³ depending on particle size and angularity (Martens & Goldmann, 2016; Schaeffer, 2020). The relatively low packing efficiency observed for clear glass compared to its particle density indicates a considerable fraction of void space, which is expected for angular fragments generated by mechanical crushing.

Green Glass

Green glass showed a slightly higher bulk density of 1,366 ± 0,003 g/cm³. Literature reports that green cullet tends to exhibit somewhat higher bulk densities than flint cullet, often by 0,02–0,05 g/cm³, primarily due to differences in particle morphology rather than intrinsic composition (Lebullenger et al., 2019). The marginally higher value observed here is therefore consistent with expectations. However, the difference between clear and green samples in this study remains small, confirming that bulk density is more strongly governed by particle size distribution and shape than by chemical composition.

Comparison with Literature

Bulk densities reported for crushed soda-lime glass typically range between 1,2 and 1,5 g/cm³ (*FEVE-Brochure-Recycling-Why-Glass-Always-Has-a-Happy-CO2-Ending*, n.d.; Martens & Goldmann, 2016). The present results fall within this interval, confirming their validity. Values closer to the upper end of the range are often associated with finer and more regularly shaped cullet, whereas lower values occur in coarser, irregularly fractured material.

Relevance for Recycling

From a recycling perspective, bulk density is a practical parameter that affects storage, transport, and dosing in batch preparation. Higher bulk density allows more efficient use of container and silo volume, while lower values imply greater void content and reduced flowability. The results of this study underline that, although particle density is chemically fixed, bulk density is highly dependent on comminution and handling conditions, which should be considered when designing recycling processes.

5.4. Tapped Density

The tapped densities of the samples ranged between 1,35 and 1,42 g/cm³, which are higher than the corresponding bulk densities (≈1,33–1,37 g/cm³). This outcome was expected, since repetitive tapping reduces interparticle void volume and promotes denser packing of the cullet without altering the intrinsic particle density.

Clear Glass

For clear glass, the tapped density was determined as 1,346 ± 0,005 g/cm³. Compared to its bulk density of 1,327 g/cm³, this represents a slight increase. Literature reports tapped densities for soda-lime flint glass cullet in the range of 1,3–1,4 g/cm³ depending on grain size and angularity (Martens & Goldmann, 2016). The result therefore falls within expected values. The relatively modest increase after tapping suggests that the loosely packed clear glass fragments already exhibited relatively efficient packing due to their angular particle shapes.

Green Glass

Green glass showed a tapped density of 1,421 ± 0,006 g/cm³, slightly higher than the value observed for clear glass. This represents an increase compared to its bulk density of 1,366 g/cm³. Literature notes that green cullet often achieves somewhat higher tapped densities than flint cullet, in the range of 1,35–1,45 g/cm³ (Lebullenger et al., 2019; Martens & Goldmann, 2016). This trend is attributed not to intrinsic density differences but to variations in particle morphology and size distribution that allow more efficient packing under vibration.

Comparison and Recycling Relevance

The differences between clear and green glass in tapped densites were minimal, confirming that compaction behaviour is primarily governed by particle morphology and size rather than chemical composition. From a recycling perspective, tapped density is a practical parameter because it reflects the maximum achievable packing of cullet during storage, silo filling, and dosing into melting furnaces. Higher tapped density implies more efficient use of silo capacity and smoother flow characteristics. The results of this study (≈1,35–1,42 g/cm³) are consistent with the industrial expectation for soda-lime cullet, further validating the representativeness of the samples.

5.5. Porosity

The porosity values determined with the manual density method (ε_{clear} = 0,421 ± 0,003, ε_{green} = 0,408 ± 0,003) indicate that approximately 40 % of the packed bed volume is void space. These results are in very good agreement with literature values for random loose packing of irregular particles, which typically range between 0,40 and 0,45 (Onoda & Liniger, 1990), While random close packing tends to

yield lower values around 0,36–0,39 (Zou & Yu, 1995). This alignment confirms the reliability of the manual approach for describing the packing structure of crushed glass. The slightly lower porosity observed for green glass suggests denser packing, which may be related to smoother fracture surfaces and less angularity compared to clear glass. Even though the absolute difference is small, this trend is consistent with previous findings that particle shape and surface morphology directly influence packing density (Zou & Yu, 1995).

In contrast, the porosity values estimated from the fluidized bed experiments via the Ergun equation did not converge to realistic values. Several measurement points showed pressure drops of $\Delta p = 0$, even at higher superficial gas velocities, indicating that the airflow bypassed parts of the bed through preferential channels rather than fluidizing it uniformly. This type of behaviour is well known for coarse, irregular, and angular particles that tend to interlock and create bridging effects, thereby preventing homogeneous expansion (Kunii & Levenspiel, 2012). As a consequence, the calculated porosities fluctuated between unrealistically low values (≈0,07–0,16) and never reached the stable equilibrium that would normally characterise true fluidization. These observations confirm that the fluidized bed method is not suitable for quantitative porosity determination of crushed glass.

Still, the experiments remain useful as a qualitative demonstration. The unstable pressure profiles and the occurrence of partial fluidization highlight the limitations of applying standard fluidization models such as the Ergun equation to real recycling materials. Similar limitations have been emphasised in the fluidization literature, where irregular particles consistently show poor fluidization performance (Kunii & Levenspiel, 2012). From a practical standpoint, this means that recycling operations involving fluidized beds—such as thermal or chemical cleaning—cannot rely on untreated cullet alone. Stable operation would require pre-treatment (e.g., sieving to narrow fractions, removal of fines, or mechanical rounding) or additional techniques such as vibration. Thus, while density-based porosity measurements provide robust data for static characterization, the fluidized bed results reveal important process constraints under dynamic conditions and therefore complement the overall assessment of cullet behaviour in recycling.

Summary

Glass recycling plays a decisive role in advancing sustainable resource management. As one of the few materials that can be recycled infinitely without a loss in quality, glass contributes both to environmental protection and to the efficiency of industrial production. Nevertheless, the recycling of container glass is not without challenges. Effective sorting, removal of impurities, and preparation of suitable particle sizes are critical to ensure high yields and furnace-ready quality. Against this background, the present thesis investigates the preparation and characterization of clear and green post-consumer glass, establishing standardised cullet for use in future optical sorting research.

The experimental work followed a systematic sequence: collection and cleaning of post-consumer bottles, manual pre-crushing, further size reduction using laboratory-scale crushers, and sieving to obtain defined size fractions. In particular, a target range of 4–10 mm was emphasised, as this is recognized as optimal for optical colour sorting systems. Comparative tests revealed that manual hammer crushing generated highly irregular fragments and oversized particles, while the jaw crusher provided reproducible results. Narrow gap settings, however, produced excessive fines, which are undesirable in recycling because they are lost and poorly detected in sorting systems. Wider gaps (5–7 mm) produced a more balanced particle size distribution and reduced dust formation. Cutting mill trials showed that splintered and elongated fragments, as well as high dust content, limit the suitability of this method for producing standardised cullet.

In addition to particle size analysis, key physical properties were evaluated. Measurements of particle, bulk, and tapped density confirmed the classification of both clear and green glass as soda-lime silicate compositions, consistent with literature values. Derived porosity values indicated that roughly 40% of the packed bed volume is void space, in agreement with expected ranges for randomly packed irregular particles. Differences between clear and green glass were small but indicated that green glass fragments can achieve slightly denser packing due to smoother fracture surfaces. Flowability tests with a vibrating chute further confirmed that the prepared cullet could be continuously transported without blockages, demonstrating compatibility with gravity-fed systems commonly used in industry.

Fluidized bed experiments were also conducted to estimate porosity dynamically. However, the results proved unsuitable for quantitative determination: pressure drop values fluctuated and in some cases fell to zero, showing that irregular, angular cullet could not be fluidized uniformly. This finding reflects a broader industrial limitation, as fluidized bed processes for cullet cleaning or treatment are difficult to apply without pre-conditioning or technical assistance such as vibration.

The combined results highlight how both the crushing method and particle properties affect downstream recycling processes. Fine fractions from narrow jaw gaps or cutting mills reduce sorting efficiency and increase material losses, while controlled fragmentation within the 4–10 mm range is most favourable. At the same time, the measured densities and porosities confirm that the cullet behaves in line with soda-lime glass standards, supporting its suitability for remelting.

By establishing reproducible methods for cullet preparation and systematically characterising its physical properties, this thesis provides a solid foundation for future academic research on optical colour sorting. Beyond its academic contribution, the work also emphasises practical insights that are relevant for industry: reducing fines, ensuring controlled particle size ranges, and understanding flow and packing behaviour are all crucial steps in making glass recycling processes more precise, efficient, and scalable.

Practical Guideline for Prepared Cullet in summary

1. Collection & Cleaning
   - Gather clear and green container glass.
   - Remove labels and residues with hot water and dish soap.
   - Ensure complete drying before further processing.
2. Pre-Crushing
   - Break bottles manually with a hammer to reduce bulk size.
   - Work inside a protective container to minimize losses.
3. Mechanical Crushing
   - Process the fragments with a jaw crusher set to a 7 mm gap.
   - Avoid narrow gaps (2,5 mm), which generate too many fines.
   - Cutting mills may be used but are less suitable due to dust and splinters.
4. Sieving & Classification
   - Use a sieving tower (e.g., 4–10 mm) to obtain standardised fractions.
   - Keep material between 4–10 mm; discard fines <4 mm and oversize >10 mm.
   - Apply a riffle splitter for representative subsamples.
5. Characterization
   - Verify particle density (pycnometer recommended), bulk and tapped densities.
   - Calculate porosity (~0,40–0,42 expected for cullet).
   - Check flowability with a vibrating chute to ensure transportability.
6. Final Output
   - Deliver a standardised cullet fraction (4–10 mm) that meets soda-lime standards.
   - The prepared cullet consists of ~95% clear glass and 5% green glass, reflecting typical recycling input streams.
   - The prepared cullet is ready to use for laboratory-scale optical colour sorting system and is suitable for remelting processes.

References

Abdelouas, A., Neeway, J., & Grambow, B. (2019). Chemical Durability of Glasses. In J. D. Musgraves, J. Hu, & L. Calvez (Eds.), *Springer Handbook of Glass*. Springer International Publishing. https://doi.org/10.1007/978-3-319-93728-1

Bevington, P. R., & Robinson, D. K. (2003). *Data reduction and error analysis for the physical sciences* (3. ed., [Nachdr.]). McGraw-Hill.

Binder+Co AG. (2021). *CLARITY optical sorting systems. Binder+Co AG*. Binder+Co AG. https://www.binder-co.com

Blanc, E. C. (1928). Backenbrecher. In E. C. Blanc, *Technologie der Brecher, Mühlen und Siebvorrichtungen* (pp. 16–50). Springer Berlin Heidelberg. https://doi.org/10.1007/978-3-642-50793-9_2

Chopinet, M.-H. (2019). History of Glass. In J. D. Musgraves, J. Hu, & L. Calvez (Eds.), *Springer Handbook of Glass*. Springer International Publishing. https://doi.org/10.1007/978-3-319-93728-1

Cicconi, M. R., & Neuville, D. R. (2019). Natural Glasses. In J. D. Musgraves, J. Hu, & L. Calvez (Eds.), *Springer Handbook of Glass*. Springer International Publishing. https://doi.org/10.1007/978-3-319-93728-1

Clare, A. G., Wachtel, P. F., & Musgraves, J. D. (2019). Halide Glasses. In J. D. Musgraves, J. Hu, & L. Calvez (Eds.), *Springer Handbook of Glass*. Springer International Publishing. https://doi.org/10.1007/978-3-319-93728-1

DIN 1319-3:1996 – Grundlagen der Messtechnik – Teil 3: Auswertung von Messungen einer einzelnen Messgröße und von mehreren Messgrößen derselben Art. (1996). Deutsches Institut für Normung e.V.

DIN EN ISO 12154:2014 – Determination of density by gas pycnometry (ISO 12154:2014). (2014). Deutsches Institut für Normung e.V.

Doremus, R. H. (1994). *Glass science* (2nd ed). J. Wiley & sons.

European Commission. (2018, May 30). *Packaging and Packaging Waste Directive (PPWD)—Directive (EU) 2018/852*. Publications Office of the European Union. eur-lex.europa.eu/legal-content/EN/TXT/?uri=celex:32018L0852

Feller, S. (2019). Borate Glasses. In J. D. Musgraves, J. Hu, & L. Calvez (Eds.), *Springer Handbook of Glass*. Springer International Publishing. https://doi.org/10.1007/978-3-319-93728-1

FEVE-brochure-Recycling-Why-glass-always-has-a-happy-CO2-ending. (n.d.).

Hupa, L., Wang, X., & Eqtesadi, S. (2019). Bioactive Glasses. In J. D. Musgraves, J. Hu, & L. Calvez (Eds.), *Springer Handbook of Glass*. Springer International Publishing. https://doi.org/10.1007/978-3-319-93728-1

International Organization for Standardization. (2014). *ISO 12154:2014 Determination of density of solids—Gas pyknometer method* (No. ISO 12154:2014). https://www.iso.org/standard/53552.html

International Organization for Standardization. (2025). *ISO 1183-1:2025 Plastics—Methods for determining the density of non-cellular plastics—Part 1: Immersion method, liquid pycnometer method and titration method* (No. ISO 1183-1:2025). https://www.iso.org/standard/53312.html

KERN & SOHN GmbH. (2022). *Operating Manual: Analytical Balance EW*. KERN & SOHN GmbH.

Kunii, D., & Levenspiel, O. (2012). *Fluidization engineering* (2. ed., reprinted). Elsevier ; Butterworth-Heinemann.

Le Bourhis, E. (2008). *Glass: Mechanics and technology*. Wiley-VCH.

Le Losq, C., Cicconi, M. R., Greaves, G. N., & Neuville, D. R. (2019). Silicate Glasses. In J. D. Musgraves, J. Hu, & L. Calvez (Eds.), *Springer Handbook of Glass*. Springer International Publishing. https://doi.org/10.1007/978-3-319-93728-1

Lebullenger, R., Mear, F. O., & Chopinet, M.-H. (2019). Glass Recycling. In J. D. Musgraves, J. Hu, & L. Calvez (Eds.), *Springer Handbook of Glass*. Springer International Publishing. https://doi.org/10.1007/978-3-319-93728-1

Martens, H., & Goldmann, D. (2016). *Recyclingtechnik: Fachbuch für Lehre und Praxis*. Springer Fachmedien Wiesbaden. https://doi.org/10.1007/978-3-658-02786-5

Munoz, F., Rocherulle, J., Ahmed, I., & Hu, L. (2019). Phosphate Glasses. In J. D. Musgraves, J. Hu, & L. Calvez (Eds.), *Springer Handbook of Glass*. Springer International Publishing. https://doi.org/10.1007/978-3-319-93728-1

Onoda, G. Y., & Liniger, E. G. (1990). Random loose packings of uniform spheres and the dilatancy onset. *Physical Review Letters*, *64*(22), 2727–2730. https://doi.org/10.1103/PhysRevLett.64.2727

Pelletier, J.-M., & Qiao, J. (2019). Metallic Glasses. In J. D. Musgraves, J. Hu, & L. Calvez (Eds.), *Springer Handbook of Glass*. Springer International Publishing. https://doi.org/10.1007/978-3-319-93728-1

Peukert, D., Xu, C., & Dowd, P. (2022). A Review of Sensor-Based Sorting in Mineral Processing: The Potential Benefits of Sensor Fusion. *Minerals*, *12*(11), 1364. https://doi.org/10.3390/min12111364

Retsch GmbH. (2025a, July 4). *AS 200 CONTROL VIBRATIONSSIEBMASCHINE*. Online document. https://www.retsch.de/de/produkte/sieben/siebmaschinen/as-200-control/

Retsch GmbH. (2025b, July 4). *BB 200 Jaw Crusher*. Online document. https://www.retsch.com/products/milling/jaw-crushers/bb-200/

Schaeffer, H. A. (with Langfeld, R.). (2020). *Werkstoff Glas: Alter Werkstoff Mit Großer Zukunft* (2nd ed). Springer Berlin / Heidelberg.

Schneider, J., Kuntsche, J., Schula, S., Schneider, F., & Wörner, J.-D. (2016). *Glasbau*. Springer Berlin Heidelberg. https://doi.org/10.1007/978-3-540-68927-0

Sesotec GmbH. (2023). *K9 glass sorting system product sheet*. Sesotec GmbH,. https://www.sesotec.com

Shelby, J. E. (2005). *Introduction to glass science and technology* (2nd ed). Royal Society of Chemistry.

Stieß, M. (1997). *Mechanische Verfahrenstechnik 2*. Springer Berlin Heidelberg. https://doi.org/10.1007/978-3-662-08599-8

Stieß, M. (2009). *Mechanische Verfahrenstechnik—Partikeltechnologie 1*. Springer Berlin Heidelberg. https://doi.org/10.1007/978/3-540-32552-9

Suibo Machinery. (2022). *AC1200 optical sorting machine brochure*. Suibo Machinery. https://www.suibomachinery.com

Thomé-Kozmiensky, K. J., & Hoffmann, B. (2010). Mechanische Aufbereitung von Abfällen. In *Recycling und Rohstoffe. 3*. TK Verl. Thomé-Kozmiensky.

UNEP (Ed.). (2024). *Beyond an age of waste: Turning rubbish into a resource*. UNEP.

Varshneya, A. K. (1994). *Fundamentals of inorganic glasses*. Academic press.

Verein Deutscher Ingenieure. (2013). *VDI-Wärmeatlas* (11., bearb. und erw. Aufl). Springer Vieweg. https://doi.org/10.1007/978-3-642-19981-3

Yao, Z., Qin, B., Huang, Z., Ruan, J., & Xu, Z. (2021). Green Combined Resource Recycling System for the Recycling of Waste Glass. *ACS Sustainable Chemistry & Engineering*, *9*(21), 7361–7368. https://doi.org/10.1021/acssuschemeng.1c01797

Zou, R. P., & Yu, A. B. (1995). The packing of spheres in a cylindrical container: The thickness effect. *Chemical Engineering Science*, *50*(9), 1504–1507. https://doi.org/10.1016/0009-2509(94)00483-8

Appendix

Table 13: Particle size distribution data for jaw crusher at 2,5mm gap widths.

x	m_o in g	m_e in g	m_{glass} in g	mass fraction	$\bar{x}$	Q_3	dx	q_3
0,000	346,810	1216,440	869,630	0,974		0,974		
					2,000		4,000	0,244
4,000	492,760	501,730	8,970	0,010		0,984		
					4,250		0,500	0,020
4,500	423,580	427,750	4,170	0,005		0,989		
					4,750		0,500	0,009
5,000	478,090	483,100	5,010	0,006		0,995		
					5,300		0,600	0,009
5,600	453,860	456,180	2,320	0,003		0,997		
					6,150		1,100	0,002
6,700	433,010	434,500	1,490	0,002		0,999		
					8,350		3,300	0,001
10,000	469,430	470,500	1,070	0,001		1,000		
		sum	892,660	1,000				

Table 14: Particle size distribution data for jaw crusher at 5mm gap widths.

x	m_o in g	m_e in g	m_{glass} in g	mass fraction	$\bar{x}$	Q_3	dx	q_3
0,000	346,810	353,730	6,920	0,047		0,047		
					2,000		4,000	0,012
4,000	492,760	515,800	23,040	0,157		0,205		
					4,250		0,500	0,315
4,500	423,580	450,790	27,210	0,186		0,391		
					4,750		0,500	0,372
5,000	478,090	507,930	29,840	0,204		0,594		
					5,300		0,600	0,340
5,600	453,860	480,070	26,210	0,179		0,773		
					6,150		1,100	0,163
6,700	433,010	466,170	33,160	0,227		1,000		
					8,350		3,300	0,069

10,000	469,430	469,430	0,000	0,000		1,000		
		ges	146,380	1,000				

Table 15: Particle size distribution data for jaw crusher at 7mm gap widths.

x	m_o in g	m_e in g	m_{glass} in g	mass fraction	$\bar{x}$	Q_3	dx	q_3
0,000	346,810	494,960	148,150	0,251		0,251		
				0,000	2,000		4,000	0,063
4,000	492,760	507,500	14,740	0,025		0,276		
				0,000	4,250		0,500	0,050
4,500	423,580	448,090	24,510	0,041		0,317		
				0,000	4,750		0,500	0,083
5,000	478,090	506,360	28,270	0,048		0,365		
				0,000	5,300		0,600	0,080
5,600	453,860	504,800	50,940	0,086		0,451		
				0,000	6,150		1,100	0,078
6,700	433,010	543,640	110,630	0,187		0,639		
				0,000	8,350		3,300	0,057
10,000	469,430	682,800	213,370	0,361		1,000		
		ges	590,610	1,000				

Table 16: Particle size distribution data for cutting mill with 20mm sieve (batch 1).

x	m_o in g	m_e in g	m_{glass} in g	mass fraction	$\bar{x}$	Q_3	dx	q_3
0,000	346,810	688,800	341,990	0,506		0,506		
				0,000	2,000		4,000	0,126
4,000	492,760	540,940	48,180	0,071		0,577		
				0,000	4,250		0,500	0,143
4,500	423,580	477,650	54,070	0,080		0,657		
				0,000	4,750		0,500	0,160
5,000	478,090	538,160	60,070	0,089		0,746		
				0,000	5,300		0,600	0,148
5,600	453,860	527,000	73,140	0,108		0,854		
				0,000	6,150		1,100	0,098
6,700	433,010	520,680	87,670	0,130		0,984		

				0,000	8,350		3,300	0,039
10,000	469,430	480,250	10,820	0,016		1,000		
		ges	675,940	1,000				

Table 17: Particle size distribution data for cutting mill with 20mm sieve (batch 2).

x	m_o in g	m_e in g	m_{glass} in g	mass fraction	$\bar{x}$	Q_3	dx	q_3
0,000	346,810	602,450	255,640	0,439		0,439		
					2,000		4,000	0,110
4,000	492,760	535,480	42,720	0,073		0,513		
					4,250		0,500	0,147
4,500	423,580	474,230	50,650	0,087		0,600		
					4,750		0,500	0,174
5,000	478,090	534,370	56,280	0,097		0,696		
					5,300		0,600	0,161
5,600	453,860	525,030	71,170	0,122		0,819		
					6,150		1,100	0,111
6,700	433,010	515,270	82,260	0,141		0,960		
					8,350		3,300	0,043
10,000	469,430	492,720	23,290	0,040		1,000		
		ges	582,010	1,000				

Table 18: Particle size distribution data for jaw-crushed clear glass at 7mm gap widths.

x	m_o in g	m_e in g	m_{glass} in g	mass fraction	$\bar{x}$	Q_3	dx	q_3
0,000	436,970	438,970	2,000	0,007		0,007		
					2,000		4,000	0,002
4,000	487,740	501,770	14,030	0,052		0,060		
					4,250		0,500	0,105
4,500	423,620	447,610	23,990	0,090		0,150		
					4,750		0,500	0,179
5,000	479,570	507,100	27,530	0,103		0,252		
					5,300		0,600	0,171
5,600	453,840	523,630	69,790	0,261		0,513		
					6,150		1,100	0,237

6,700	432,990	554,290	121,300	0,453		0,966		
					8,350		3,300	0,137
10,000	469,360	475,180	5,820	0,022		0,988		
					10,600		1,200	0,018
11,200	395,130	398,350	3,220	0,012		1,000		
		ges	267,680	1,000				

Table 19: Particle size distribution data for jaw-crushed green glass at 7mm gap widths.

x	m_o in g	m_e in g	m_{glass} in g	mass fraction	$\bar{x}$	Q_3	dx	q_3
0,000	436,970	437,560	0,590	0,002		0,002		
					2,000		4,000	0,001
4,000	487,730	509,560	21,830	0,082		0,084		
					4,250		0,500	0,163
4,500	423,600	463,010	39,410	0,147		0,231		
					4,750		0,500	0,294
5,000	479,620	523,190	43,570	0,163		0,394		
					5,300		0,600	0,271
5,600	453,840	531,540	77,700	0,290		0,684		
					6,150		1,100	0,264
6,700	432,990	566,730	133,740	0,500		1,184		
					8,350		3,300	0,151
10,000	469,350	475,530	6,180	0,023		1,207		
					10,600		1,200	0,019
11,200	395,130	395,130	0,000	0,000		1,207		
		ges	323,020	1,207				

Table 20: Empty column measurement (baseline) for the fluidized bed setup.

Float Body in mm	Volumetric Flow in l/min	Δh in mm	Δp in Pa	$\bar{w}$ in m/s
6,000000	2,215300	17,000000	166,770000	0,002398
14,000000	3,714587	28,000000	274,680000	0,004022
27,000000	4,626161	45,000000	441,450000	0,005009
63,000000	7,063354	104,000000	1020,240000	0,007647

89,000000	14,141547	152,000000	1491,120000	0,015311
120,000000	19,802192	220,000000	2158,200000	0,021440
150,000000	30,715977	292,000000	2864,520000	0,033256
200,000000	49,980645	440,000000	4316,400000	0,054113